

**EFFECT OF VISUAL STIMULI WITH  
FEARFUL EMOTIONAL CUE ON  
POPULATION RECEPTIVE FIELD  
ESTIMATES**

A THESIS SUBMITTED TO  
THE GRADUATE SCHOOL OF ENGINEERING AND SCIENCE  
OF BILKENT UNIVERSITY  
IN PARTIAL FULFILLMENT OF THE REQUIREMENTS FOR  
THE DEGREE OF  
MASTER OF SCIENCE  
IN  
NEUROSCIENCE

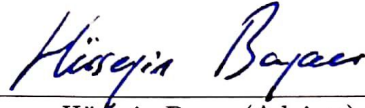
By  
Cemre Yilmaz  
July 2019

EFFECT OF VISUAL STIMULI WITH FEARFUL EMOTOINAL  
CUE ON POPULATION RECEPTIVE FIELD ESTIMATES

By Cemre Yilmaz

July 2019

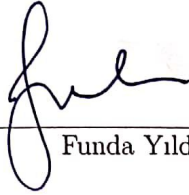
We certify that we have read this thesis and that in our opinion it is fully adequate,  
in scope and in quality, as a thesis for the degree of Master of Science.



Hüseyin Boyacı(Advisor)

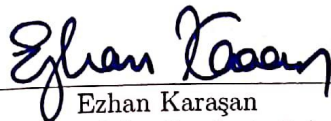


H. Hulusi Kafalgönül



Funda Yıldırım

Approved for the Graduate School of Engineering and Science:



Ezhan Karahan  
Director of the Graduate School

## ABSTRACT

# EFFECT OF VISUAL STIMULI WITH FEARFUL EMOTIONAL CUE ON POPULATION RECEPTIVE FIELD ESTIMATES

Cemre Yılmaz

M.S. in Neuroscience

Advisor: Hüseyin Boyacı

July 2019

Previous studies showed that the content of stimulus might affect the results of population receptive field (pRF) estimation method [1, 2, 3]. In addition, emotion might modulate visual processing in humans by increasing BOLD activity [4, 5]. Taken together, the stimulus with emotional cue might affect the pRF parameters. To investigate the effect of emotion on visual processing, we used the population receptive field (pRF) method [6], with simultaneous wedge and ring stimuli rendered with scrambled, neutral or emotional images. Results showed that the pRF estimations were affected by the stimulus content in visual areas hV4 and V3A, as well as lower retinotopic regions: V1, V2 and V3. Moreover, we showed the emotional content of stimulus might lead to the increased pRF sizes as well as a shift in pRF centers toward the eccentric side. We argue that the increased pRF size and the pRF shift might be a result of emotional modulation of visual processing.

*Keywords:* Neuroimaging, emotional studies, fMRI, population receptive field estimation, pRF.

## ÖZET

# KORKU DUYGUSU İÇEREN GÖRSEL UYARANLARIN POPÜLASYON ALICI ALAN TAHMİNLERİ UZERİNDEKİ ETKİSİ

Cemre Yılmaz

Nörobilim, Yüksek Lisans

Tez Danışmanı: Hüseyin Boyacı

Temmuz 2019

Önceki çalışmalar, uyaran içeriğinin popülasyon alıcı alan (pAA) tahmin yöntemi sonuçlarına etki edebileceğini göstermiştir [1, 2, 3]. Ayrıca, duygu, insanlarda BOLD aktivitesini arttırarak görsel işlemeyi düzenleyebilir [4, 5]. Bütün bunlar ele alındığında, duygusal içerikli uyaranlar pAA parametrelerinde değişikliğe yol açabilir. Duygunun görsel işleme üzerindeki etkisini daha detaylı araştırmak için, Dumoulin ve Wandell tarafından 2008'deki makalelerinde açıklanmış pAA tahmin yöntemini, içerisinde görseller yerleştirilmiş, eş zamanlı pasta dilimi ve halka uyararı ile kullandık [6]. Sonuçlarımız, uyaran içeriğinin pAA tahminlerine hV4 ve V3A bölgelerinin yanı sıra daha ilksel bölgeler olan V1, V2 ve V3'te de etki edebildiğini gösterdi. Ayrıca, uyarandaki duygu içeriğinin büyük pAA boyutu ile pAA merkezinde daha dışsal alanlara kaymaya yol açabildiği bulduk. Daha büyük pAA ile pAA merkezindeki kaymanın, görsel işleme üzerinde duygunun düzenleyici işlevinin bir sonucu olduğunu öne sürüyoruz.

*Anahtar sözcükler:* Beyin görüntüleme, duygu çalışmaları, iMRG, popülasyon alıcı alanı tahmini, pAA.

## Acknowledgement

I would like to state that I am very grateful for Olcay Yılmaz, my husband, for his emotional, intellectual and financial support during this project. And, I would like to thank my brother, Eray Topcu for his patience while tirelessly listening my dead-ends and his suggestions to find out the solution. Then, I am thankful to my mom, Sevgi Şerbetci for her endless moral support.

I would like to express my gratitude to my thesis advisor, Assoc. Prof. Dr. Hüseyin Boyacı, for his constructive comments and academic guidance during my graduate study. I would also like to thank the other members of my examining committee, Asst. Prof. Dr. H. Hulusi Kafalgönül and Asst. Prof. Dr. Funda Yıldırım, for their contributions and valuable suggestions.

I owe my special thanks to Didem Gökçay who helped to start my journey as a neuroscientist for her friendly encouragement and guidance. I am also very thankful to have such a lovely friends Batuhan Erkat, Ecem Altan, Dilara Erişen, Cem Benar, Görkem Er, Hossein Mehrzadfar, Beyza Akkoyunlu, Buse Merve Ürgen in the lab environment. Their contributions to this study are immeasurable.

Last but not least, I thank all the people who spent their time and endured the long MR scans to participate this study.

# Contents

<b>1</b>	<b>Introduction</b>	<b>1</b>
1.1	Connectivity in Visual System . . . . .	1
1.2	Mapping the Visual Cortex . . . . .	7
1.3	Cognitive Studies on Receptive Fields . . . . .	11
1.4	Effect of Emotional Content on pRF . . . . .	13
<b>2</b>	<b>Methods</b>	<b>15</b>
2.1	Participants . . . . .	15
2.2	Stimuli Presentation . . . . .	15
2.3	Experimental Protocol and MR Image Acquisition . . . . .	17
2.4	Analysis . . . . .	19
2.4.1	Preprocessing of MR Data . . . . .	19
2.4.2	Analysis of the Response to Fixation Task . . . . .	20
2.4.3	pRF Estimation . . . . .	21

2.4.4	Analysis of Image Properties . . . . .	23
<b>3</b>	<b>Results</b>	<b>24</b>
3.1	The Effect of Image Coherence . . . . .	24
3.1.1	The Size of Maps . . . . .	24
3.1.2	The Change in pRF Estimations . . . . .	27
3.2	The Effect of Emotion . . . . .	32
3.2.1	The Size of Maps . . . . .	32
3.2.2	The Change in pRF Estimations . . . . .	34
3.3	Fixation Task . . . . .	39
3.4	Hemispheric Asymmetry . . . . .	40
3.5	Image Properties . . . . .	42
<b>4</b>	<b>Discussion</b>	<b>46</b>
4.1	The coherent image is better for pRF mapping . . . . .	47
4.2	Emotional content of stimulus might lead to an increased pRF size	48
4.3	pRF sizes are larger in the right hemisphere than in the left hemisphere . . . . .	50
4.4	Conclusion . . . . .	51
4.5	Limitations . . . . .	52
4.6	Future directions . . . . .	52

<b>A Behavioral Test for Image Recognition</b>	<b>62</b>
<b>B Saliency Maps of Images</b>	<b>65</b>
<b>C Within-Subject Results</b>	<b>71</b>
C.1 Subject 1 . . . . .	72
C.2 Subject 2 . . . . .	76
C.3 Subject 3 . . . . .	80
C.4 Subject 4 . . . . .	84
C.5 Subject 5 . . . . .	88



# List of Figures

1.1	Illustration of labelled lines on the visual system . . . . .	4
1.2	Retinotopic map of visual cortex at right hemisphere. . . . .	9
2.1	Representation of stimulus in the experiment . . . . .	17
2.2	Order of stimulus in the experiment . . . . .	18
3.1	Representative maps of emotional and scrambled conditions . . . .	26
3.2	Descriptive plot of pRF sizes estimated for scrambled and emotional conditions . . . . .	28
3.3	Radial map of pRF centers calculated for scrambled and emotional conditions . . . . .	30
3.4	Representative maps of emotional and neutral conditions . . . . .	33
3.5	pRF sizes estimated for neutral and emotional conditions . . . . .	35
3.6	Radial map of pRF centers calculated for neutral and emotional conditions . . . . .	37
3.7	Descriptive plot of pRF sizes on left and right hemispheres . . . . .	41

3.8	Descriptive plot of the locations of pRF centers on left and right hemispheres . . . . .	42
3.9	The averaged saliency maps of conditions. . . . .	43
3.10	The averaged pRF sizes at the most salient points for each condition.	44
3.11	The averaged luminance of images in each condition. . . . .	45
B.1	The saliency maps of scrambled images . . . . .	66
B.2	The saliency maps of neutral images . . . . .	69
B.3	The saliency maps of emotional images . . . . .	70
C.1	The pRF estimates for Subject 1 . . . . .	74
C.2	Polar maps of Subject 1 . . . . .	75
C.3	The pRF estimates for Subject 2 . . . . .	78
C.4	Polar maps of Subject 2 . . . . .	79
C.5	The pRF estimates for Subject 3 . . . . .	82
C.6	Polar maps of Subject 3 . . . . .	83
C.7	The pRF estimates for Subject 4 . . . . .	86
C.8	Polar maps of Subject 4 . . . . .	87
C.9	The pRF estimates for Subject 5 . . . . .	90
C.10	Polar maps of Subject 5 . . . . .	91

# List of Tables

3.1	Number of reliable vertices on each hemisphere of each subject in emotional and scrambled conditions . . . . .	25
3.2	The results of repeated measures ANOVA between the sigma values of scrambled and emotional condition . . . . .	29
3.3	The results of repeated measures ANOVA between the pRF centers of scrambled and emotional condition . . . . .	31
3.4	The results of t-test between the beta values of scrambled and emotional condition . . . . .	32
3.5	Number of reliable vertices on each hemisphere of each subject in emotional and neutral conditions . . . . .	34
3.6	The results of repeated measures ANOVA between the sigma values of neutral and emotional condition . . . . .	36
3.7	The results of repeated measures ANOVA between the pRF centers of neutral and emotional condition . . . . .	38
3.8	The results of t-test between the beta values of neutral and emotional condition . . . . .	39
3.9	The averaged ratios of correct answers for fixation task. . . . .	40

3.10	The averaged time delay of response for fixation task. . . . .	40
A.1	The ratio of correct answers of each subjects for test of image recognition . . . . .	63
C.1	Success of Subject 1 in fixation task. . . . .	72
C.2	Precision of Subject 1 in fixation task. . . . .	73
C.3	Success of Subject 2 in fixation task. . . . .	76
C.4	Precision of Subject 2 in fixation task. . . . .	77
C.5	Success of Subject 3 in fixation task. . . . .	80
C.6	Precision of Subject 3 in fixation task. . . . .	81
C.7	Success of Subject 4 in fixation task. . . . .	84
C.8	Precision of Subject 4 in fixation task. . . . .	85
C.9	Success of Subject 5 in fixation task. . . . .	88
C.10	Precision of Subject 5 in fixation task. . . . .	89

# Chapter 1

## Introduction

### 1.1 Connectivity in Visual System

In his scratch-reflex study on dogs in 1906, Sir Charles Scott Sherrington first defined receptive field for the somatosensory system: Receptive field of a reflex was defined as the area on skin of which stimulation resulted in that reflex [7]. After decades, Haldan Keffer Hartline (1937) showed that the retinal ganglion cells of vertebrates also had receptive fields defined as an area on visual field in which a retinal ganglion cell responded the stimulus. According to his study, the location of receptive field was fixed on visual field whereas the size was affected by environmental factors [8]. In 1959, Hubel and Wiesel defined the properties of receptive fields detailed in visual cortex. They defined receptive field as retinal areas at which the stimulation would lead to a neuronal activation on the cortical area [9]. After several years, the receptive field property was proven in human visual cortex by using microelectrodes implanted into brains of people who has serious seizures [10].

With the light of forementioned studies and many others, the features of receptive fields were revealed. First, there is a common feature of center-surround

relation in receptive fields of most sensory systems (namely somatosensory, auditory and visual system; in this thesis, however, we focus on the visual system). If the stimulation of center leads to excitation of neuron and the stimulation of surround leads to inhibition of neuron, it is called *on-center/off-surround*. If this relation is in the other way, i.e. inhibitory center and excitatory surround, it is called *off-center/on-surround*. This center-surround relation was observed at the early-stages of visual system, namely on retina [11], on lateral geniculate nucleus (LGN) [12] and on the visual cortex [9]. Another feature which is important not only for understanding functionality of the visual system but also for understanding its structural connections: the increase in receptive field size through eccentricity and through hierarchy [13]. We observe the smallest receptive fields at the central area of visual field, the point on which the eyes focus or the *fovea* at which the acuity is the highest, and the size of receptive fields increases while moving away from the fovea, i.e. increasing the eccentricity. Besides, the receptive field sizes at lower visual areas such as V1, i.e. primary visual cortex, are smaller than the ones at higher visual areas such as V4. The convergent connections through the hierarchy in visual system would result in such a feature of receptive fields. To put simply, a few neurons in retina transmit the signal to one neuron in lateral geniculate nucleus (LGN) in thalamus, and a few neurons in LGN transmit the signal to one neuron in V1, and a few neurons in V1 transmit the signal to one neuron in V2, i.e. secondary visual cortex, and so on. This is called *labelled-line* and the connections are convergent through hierarchy as illustrated in Figure 1.1. As a result of this convergence, the higher visual areas process wider area and broader information.

As a result of the organization of the labelled-lines, the visual field is represented on the cortex spatially as it is, except the mapping of the visual field on the cortex is upside down and laterally inverted. This is called as *topographical representation* which is common among somatosensory, auditory and visual system; as with receptive fields. For visual system, topographical representation results in retinotopic organization on visual cortex because the visual field is fixed on retina regardless of eye movements. Therefore, the fixation point is an important

reference point while defining retinotopic regions. That is why, visual neuroscientists commonly ask subjects to look at fixation point on the screen during the experiments aiming to define retinotopic regions. Then, we can divide the visual field into two parts as right visual hemifield and left visual hemifield. It is important since their representations are generally divided between two hemispheres: The right visual hemifield is represented on left hemisphere and the left visual hemifield is represented on right hemisphere, in the early stages of visual system. The reason for the contralesionality is the crossing over at optic chiasm as shown in Figure 1.1. However, this division does not mean the absence of ipsilateral representation. There is also an information flow from right visual hemifield to right hemisphere and from left visual hemifield to left hemisphere. Additionally, the retinotopic regions at the higher levels of the hierarchy have larger receptive fields that can include the ipsilateral visual hemifield. The division of visual field between hemispheres means that the contralateral connections are more dominant than ipsilateral connections on each hemisphere.

Retinotopic regions are defined empirically by following certain criteria. First, representation of a single point on visual field should not be repeated on one retinotopic region by definition. We expect that the representation of a single point is repeated on different retinotopic regions. Second, a retinotopic region should represent a substantial part of visual field, e.g. the right visual hemifield. We expect a retinotopic region as a continuous representations. The discontinuity indicates the border of a new retinotopic region. The only exceptions are V2 and V3 for the continuity. They are divided as ventral and dorsal parts as shown in Figure 1.2. Third, the retinotopic map should form a consistent topological pattern across the individuals. This does not mean that the retinotopic maps should be the same for every subject. The anatomical deviations and differences due to the stimulus or analysis method selection are accepted. However, the retinotopic regions should have an expected adjacency. [14]

The delineation of human retinotopic regions is important for visual neuroscience theories that postulate the process for specific perceptual functions are localized on specialized cortical regions. At the posterior side, the visual cortex

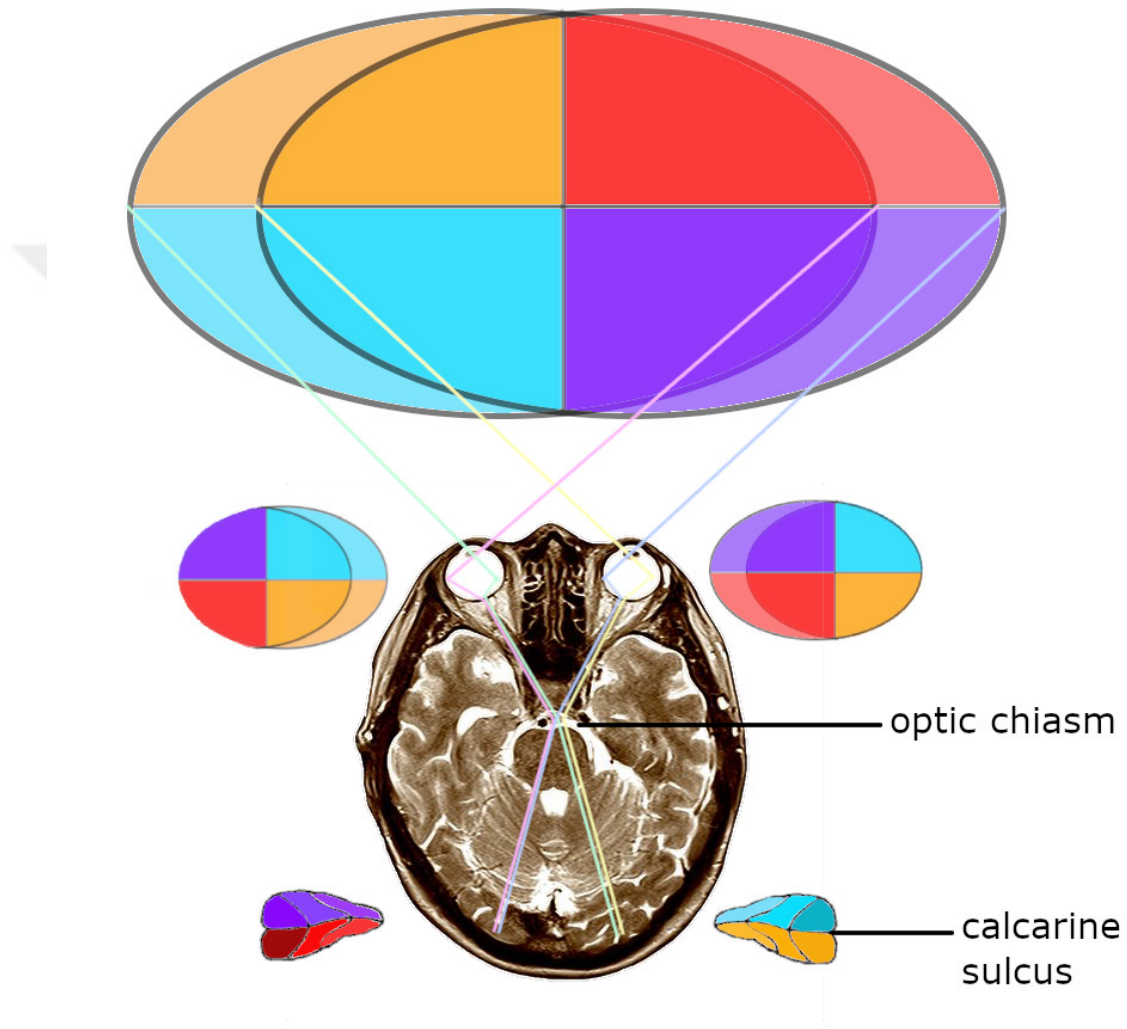


Figure 1.1: **Illustration of labelled lines on the visual system.** As illustrated on the figure, the retina of each eye gets signal from a part of the visual field. Each visual hemifield is divided into four part so that the labelled lines can be shown as color-coded. Due to the laws of optics, the visual field forms an image on the retina as upside down and laterally inverted. Such a representation remains through all levels of visual system. The nerve fibers cross over on the optic chiasm. As a result, the left hemisphere gets signal from the right visual field and the right hemisphere gets signal from left visual field. This is called contralateral connection.



is mapped as V1, V2 and V3. The horizontal line e.g. at right visual hemifield is represented approximately on Calcarine sulcus on left hemisphere. Calcarine sulcus, therefore, is an important anatomical indicator for retinotopic maps. It is generally located at the midline of V1. As we mentioned before, V2 is divided into two parts as dorsal V2 (V2d) at the dorsal side of V1 and ventral V2 (V2v) at the ventral side of V1. Similarly, dorsal V3 (V3d) is adjacent to V2d and ventral V3 (V3v) is adjacent to V2v. Human V3d is homologous to macaque V3 whereas the homologous region to human V3v is called VP in macaques. Those three retinotopic regions share a common foveal representation at the most posterior side. As shown in Figure 1.1, the horizontal line at the visual field is represented on the Calcarine sulci, i.e. the half of horizontal line in right visual hemifield is represented on left Calcarine sulcus and the other half of horizontal line in left visual hemifield is represented on right Calcarine sulcus. Through the dorsal side on the cortex, the lower parts of visual hemifield coded with blue and purple on Figure 1.1 are represented on dorsal half of V1. On the other hand, the upper parts of visual hemifield or the yellow and red parts on Figure 1.1 are represented at more ventral side of V1. Hence, the map on V1 includes one complete hemifield, which is congruent with the criteria for retinotopic regions. As a result, the map on right V1 would be represented by blue and yellow colors according to the color-coding in Figure 1.1. The dorsal part of right V1 starting from right Calcarine sulcus is represented by blue and the ventral part is represented by yellow. Similarly, the dorsal part of left V1 starting from left Calcarine sulcus is represented by purple and the ventral part is represented by red as illustrated in Figure 1.1.

Since one point in visual field must be represented only once in one retinotopic region, the border between V1 and V2 is defined as the end of map of one visual hemifield which is a vertical line on visual field. The representation of lower part of the vertical line can be defined as the border between V1 and V2d. Similarly, the border between V1 and V2v is the representation of upper part of the vertical line. Moreover, the representations on V2d and V2v are the reversal of dorsal and ventral half of V1, respectively. As a result, the representation on e.g. right V2d can be coded as blue color according to the color coding in Figure 1.1. If a

vertical line at lower part is rotating clockwise, its representation on right V2d moves towards more dorsal side from its border with V1. When the line reaches the horizontal position on left visual field, it would be represented on the border between V2d and V3d since it is known that map on V2d includes only a quarter of visual field. Therefore, the map on V2d is the mirror of map on dorsal half of V1. Similarly, the map on V2v is the mirror of map on ventral half of V1. Therefore, the V2v e.g. on right hemisphere represents the area coded with yellow according to the Figure 1.1. Hence, the border between V2v and V3v e.g. on right hemisphere is defined by the repetitive representation of horizontal line on the left visual hemifield [14].

In the visual cortex which includes the occipital lobe and some parts of parietal and temporal lobes, there are two main streams for specific perceptual functions: dorsal stream in which motion is processed and ventral stream in which object and face recognition occurs as well as color perception [15]. The dorsal stream was related to the motion perception and to the processing of spatial information of stimulus. It extends from V3d to human middle temporal (hMT). The defined retinotopic regions in dorsal stream are V3A, V3B, V6 (a.k.a. dorsomedial area) and hMT. Among them, V3A and V3B share a common foveal representation which is different than the foveal representation of V1/2/3, and V3A is adjacent to V3d whereas V3B is adjacent to V3A [16]. The foveal representation on V6 is distinct from that of V1/2/3 and also that of V3A/B. It is located in parieto-occipital sulcus. Lastly, human middle temporal area is abbreviated as hMT [17]. It is known as a highly sensitive area to motion. The maps on those areas include the representation of one complete visual hemifield. The borders can be defined by finding the borders of reversal maps of visual hemifield. [14]

The ventral stream extends from V3v to ventral occipital complex: hV4, LO-1, LO-2, VO-1 and VO-2. The ventral stream was related to object recognition and color perception. First, hV4 is adjacent to V3v and it shares common foveal representation with V1/2/3 [18]. hV4 represents more than a quarter of visual field whereas the other retinotopic areas represent generally one complete visual hemifield. There is a debate on whether or not human V4 has subdivisions similar

to the macaque V4. In macaque monkeys, V4 is divided into dorsal V4 and ventral V4 [19]. However, whether human V4 splits into dorsal and ventral parts is arguable. Human V4 is considered as homologous to ventral V4 of macaque monkeys rather than having two parts [19]. The homologue of dorsal V4 of macaque monkeys was not clearly shown yet although some regions were suggested as the homologue of macaque dorsal V4 in human visual system [18, 20]. Some retinotopic studies point to the conclusion that there might be no retinotopic region in human visual cortex homologous to dorsal V4 of macaque monkeys [19, 21]. Second, lateral occipital (LO) complex was defined as a retinotopic region and it is divided into two areas: LO-1 and LO-2. LO-1 is directly adjacent to V3d and LO-2 is adjacent to LO-1. Both regions represent the complete visual hemifield. While polar map of LO-1 is mirror of polar map of V3, polar map of LO-2 is mirror of polar map of LO-1 [14, 22]. They also share a common foveal representation with V1/2/3 and hV4. Third, ventral occipital (VO) complex is located at the ventral side of hV4. It is divided into VO-1 and VO-2. VO-1 and VO-2 has a distinct foveal representation. Both regions represent the complete visual hemifield. [14, 23]

Besides the dorsal and ventral stream, intraparietal sulcus (IPS) is defined as a retinotopic region which is related with eye movement and attentional shifts. The mapping on IPS is divided into different areas. When it was first discovered, this area was named as V7 [24]. However, after several areas were defined on IPS, V7 was called as IPS-0. IPS-0 shares a common foveal representation, which is distinct from the previously mentioned foveal representations, with IPS-1 and IPS-2. IPS-2 has a polar map reversal of IPS-1. The retinotopic regions at more anterior part are called as IPS-3 and IPS-4. [14, 25]

## 1.2 Mapping the Visual Cortex

In 1997, Stephen A. Engel and his colleagues published an article in which they described a method to identify retinotopic regions on visual cortex [26]. The method is widely known as the phase encoded method. They presented wedge

and ring stimuli to the participants while they lied down in MR scanner looking at the fixation point on screen. The wedge stimulus rotated clockwise and counter-clockwise whereas the ring stimulus expanded and shrunk, each at different runs. As the wedge rotates clockwise starting from upper ventricular meridian, the activation on e.g. V1 travels towards dorsal side. As the ring expands, the activation on visual cortex travels towards anterior side. Since it can be said that the activation “travels” along the visual cortex, this method is also called as “travelling wave”.

First, they defined the borders between visual areas V1, V2 and V3 with the aid of activation in response to wedge stimulus. To define the borders between those areas, the reversibly repetitive representation of polar map is used as shown in Figure 1.2. Polar map is created by cross-correlation of fMRI data with the location of wedge which rotates clockwise and counter-clockwise during the experiment.

The second important outcome of travelling wave method was the eccentricity map constructed by the activation in response to ring stimulus. The anterior border of retinotopic map corresponds the representation of the largest ring presented during experiment (see Figure 1.2). This is defined by using eccentricity map created by cross-correlation of fMRI data with the positions of ring which expands and shrinks during the experiment.

This method was an important development at that time. When region of interest (ROI) includes one or more retinotopic regions, the travelling wave method is very useful to define a functional ROI instead of anatomical ROI. An anatomical ROI can be helpful for some studies. On the other hand, functional connections may deviate slightly from anatomical areas, which is significantly important to define properly a retinotopic region as the ROI in a study. That is why retinotopic mapping is important for many visual studies.

The phase-encoded method or travelling wave method is used to map retinotopic regions according to the cross-correlation of the stimulus with BOLD activity. The analysis focuses on the stimulus leading to the highest response on

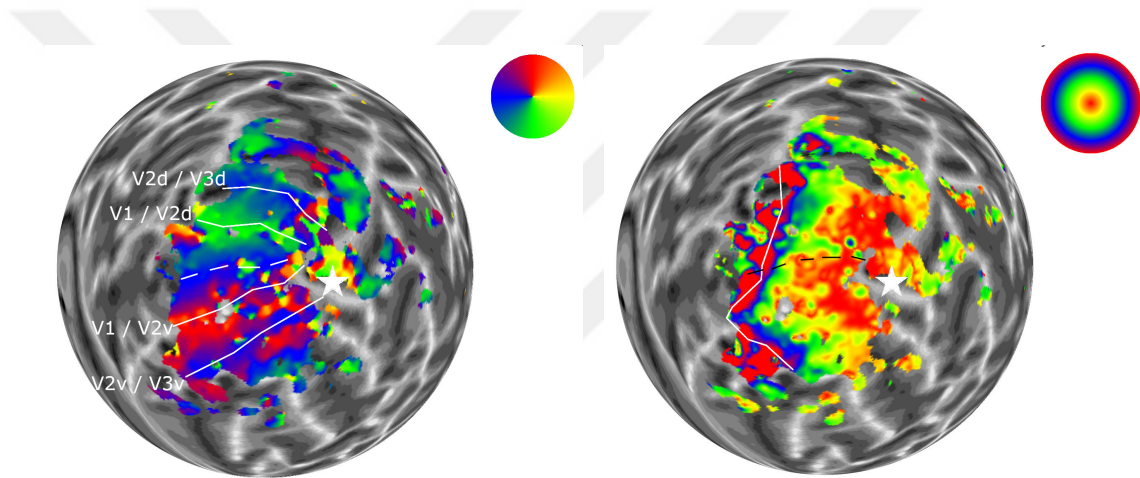


Figure 1.2: **Retinotopic map of visual cortex at right hemisphere.** (a) *The borders of retinotopic regions with respect to polar map.* The legend at the right side of image represent the locations of wedges on visual field. The white dashed line on the map represents the calcarine sulcus, the white solid lines represent the borders of retinotopic regions and the star represents the posterior side. (b) *The posterior border of retionotopic map with respect to eccentricity map.* The legend at the right side of image represent the eccentricity of rings on visual field. The white dashed line on the map represents the calcarine sulcus, the black solid line represents the border and the star represents the posterior side.

cortical areas. Therefore, certain stimulation leading to an activation on a cortical area can be neglected because an activation could not be correlated with the stimulus if it is below the highest values observed in the same cortical area. In other words, the receptive fields of a neuronal population is stimulated by a range of locations in visual field rather than by a strict location. The traveling wave method can estimate only the central area of each receptive field of population of which the stimulation would give the highest response. To overcome this shortcoming, we can estimate the response of neuronal populations to a range of locations by analyzing receptive fields of neuronal population in every voxel.

A recently developed method, the population receptive field estimation, was published by Dumoulin and Wandell in 2008 [6]. They assumed that we could model receptive field of a group of neuron in a voxel. Hence, they created a mathematical model and then, they fitted the fMRI data to this model to estimate pRF sizes and locations of populations in every voxel. Moreover, we can estimate whether the representation of stimulus is mirror or nonmirror of the stimulus, called as *field sign* estimation. As we mentioned previously, the retinotopic regions may represent the stimulus as a mirror or nonmirror representation. Hence, the field sign estimation is a useful information which improves the delineation of visual cortex. This new noninvasive method was very important for the studies on receptive field since those studies could be performed only via electrophysiology and therefore, such studies were very limited on human brain.

For pRF estimation method, Dumoulin and Wandell used drifting bars as a novel stimulus for mapping. [6] Additionally, simultaneous presentation of wedges and rings as a diverse set of stimulus from the travelling wave method was suggested for pRF studies by Alvarez and his colleagues. Concerning the best stimulus type, they showed that the drifting bar stimulus required more experimental duration than simultaneous wedge and ring stimulus to construct maps with similar goodness-of-fit by comparing these two types, drifting bars and simultaneous wedge and ring. Moreover, the reliability of model fit was higher when they used simultaneous wedge and ring stimulus, compared to the drifting bar. [27]

With pRF estimation, we can estimate the range of locations in visual field which stimulates every voxel. As a result, we can estimate polar and eccentricity maps by using the information of receptive fields of every voxel, not by using the information of the locations leading to highest response. Therefore, pRF estimation allows us not only to define visual areas but also to study on dynamic functionality of visual system via pRF sizes and locations since pRF estimations might be affected by cognitive and also by developmental processes. Another advantage of pRF estimation over travelling wave method is the increased precision. The closest point to fovea that can be mapped via travelling wave method is 2 or 3 degree of visual field at least. On the other hand, pRF estimation can go further down to or even below half a degree of visual field [6].

### 1.3 Cognitive Studies on Receptive Fields

The pRF estimation method is applicable to cognitive and developmental studies not only as a method to define functional ROIs but also as a method to study the properties of receptive field by changing the pRF model or the stimulus type. For instance, Anderson and her colleagues used pRF estimation with a model including center-surround interaction. They have shown that people with schizophrenia had reduced surround inhibition compared to the control group [28]. This finding is important to support the argument that the cause of schizophrenia might be some abnormalities in brain development before birth or in early age as suggested previously by psychophysical studies [29]. A recent study supported this developmental argument. In 2019, Dekker and her colleagues showed that pRF tuning property changed after age 6 until age 12 [30]. Therefore, we can say that pRF estimation method is useful to study in the fields of developmental and cognitive neuroscience.

Another interesting example of using pRF estimation method is the study on illusions. Dongjun He and his colleagues used Ponzo corridor and placed the ring stimulus either at the front or at the back part. The researchers defined their ROIs as V1, V2 and V3 by using travelling-wave method. For pRF estimation,

the ring stimulus with flickering high-contrast checkerboard pattern was presented on a Ponzo corridor background. In the first run, the ring was expanding at the front part of the corridor and in the second run, the ring was expanding at back part of the corridor. The third and the fourth runs included the shrinking ring at front and back parts of the corridor, respectively. Then, they estimated pRF sizes and locations on V1, V2 and V3 by using the data from the illusory experiment in which ring stimulus was expanding or shrinking with a Ponzo corridor background. As a result of their study, they concluded that the Ponzo illusion led to a shift on pRF centers towards fovea resulted from the information of ring at the back. [3]

In another study, Benjamin de Haas and his colleagues presented the stimulus perceived as a bar in a similar way with Kanizsa illusion. As Gaetano Kanizsa explained in his paper, we can see illusory contours in certain conditions [31]. The most famous Kanizsa illusion is the illusory triangle perceived due to three pacmans. We perceive a white triangle on top of three black disks at each corner although there is no physical contours [31]. In the study of de Haas and his colleagues, a gray bar was drifting on a gray square with a brick wall background. In the first condition, the hue of bar and square was same, which was the Kanizsa condition. The bar was perceived due to illusory contours on the gray square. In the second and third condition, the bar was darker than the square. The bar was perceived as behind the square in the second condition, which was called as occlusion condition, and it was perceived as in front of square in the third condition, which was called as luminance condition. The estimated pRF sizes for Kanizsa-illusory condition was smaller than the other conditions. Moreover, the pRF maps of three conditions were dramatically smaller than a typical pRF map, such that a reliable delineation was not possible using polar maps. Therefore, we can say that the context of stimulus may affect the estimations of pRF method as well as the reliability of the estimations. [2]

Besides the contextual features, the low-level features of stimulus were also discussed in previous studies. The pRF sizes estimated using orientation-contrast pattern (with low luminance-contrast) created by small gabor patches were shown to be smaller than the pRF sizes estimated by using high luminance-contrast



checkerboard pattern [1]. On the other hand, the chromatic checkerboard pattern showed no significant difference than monochromatic one [32]. So, changing the stimulus features, e.g. context or contrast can affect the resulting estimations of pRF size.

## 1.4 Effect of Emotional Content on pRF

Since the content of stimulus can affect the pRF estimations, we focused on the effects of stimulus content. The emotional content of stimulus might affect the estimations of pRF size considering the previous pRF studies and emotion studies.

The presentation of stimuli having an emotional cue might result in increased BOLD activation on visual cortex [4]. Although it is commonly thought the effect of negative emotions are stronger than that of the positive emotions, there is evidence that the effect of emotion on visual cortex is not related to its valence, different than the prefrontal cortex at which the effect of emotion is highly related to its valence [5]. Most of the emotion studies found the effect of emotional modulation on higher visual areas such as temporo-occipital. However, emotional modulation results in similar activation patterns to the attentional with some deviations. Hence, it has been suggested that the emotional and attentional modulations may use concurrent pathway but still those two are separate modulatory mechanisms [5, 33]. Since the effect of emotion on receptive field sizes and locations is not studied well, we can expect the emotional modulation might be similar to the findings of attention studies.

It has been shown that receptive fields shrink toward the attended stimulus both in a human fMRI study [34] and in electrophysiological studies conducted in monkeys [35, 36]. We can suggest that smaller pRF size leads to increased acuity since, beside from attention studies, the pRF size decreases towards fovea. We can also suggest that such a decrease in pRF size might lead to process of more detailed information about the stimulus since the same number of neurons would process decreased amount of information coming from the stimulus. Moreover,

we can note that attention might affect the low level vision although attention is commonly considered as a high level process. For example, attentional modulation can lead to increased BOLD activity in V1, V2 and V3 at the corresponding areas of eccentricity where the attentional cue was presented [37, 38]. The increased BOLD activity might not be directly related with the decreased pRF size that was shown in previous studies. However, we can conclude that the attention can modulate the visual system at low level and it can lead to a decrease in pRF size.

Considering this hypothesis that the emotion and attention modulates visual system by using concurrent pathways and some findings from electrophysiology studies that showed a direct projection from amygdala to V1 in macaque monkeys [39, 40], we argue that emotion can modulate the activity of visual cortex from the lowest level, i.e. V1 area, to the highest level, i.e. temporo-occipital lobe. To investigate further this modulatory effect of emotion, the pRF estimation method can be very useful since it might detect the possible changes in pRF profiles that might change the visual processing with an activational change undetectable with traditional subtraction protocols. We used images with fearful content and we presented those images rendered with simultaneous wedge and ring stimulus since, as we mentioned previously, it is known that the content of stimulus can affect the pRF estimations.

In the current study, we used visual stimulus with fearful content as a negative emotion to investigate the emotional modulation of visual system. The images that were selected from Nencki Affective Picture Set were rendered with simultaneous wedge and ring mask to create our stimulus set. We used pRF estimation method by using images with fearful cue and images that were emotionally neutral. Hence, we could compare the estimations for emotional and neutral conditions. We expected to find a change in pRF estimations in emotional condition compared to neutral condition. We hypothesized that the modulational effect of emotion would be observed dominantly on ventral stream rather than the retinotopic regions in dorsal stream because the previous findings showed the emotion modulated mostly the ventral retinotopic regions [4, 5].

# Chapter 2

## Methods

### 2.1 Participants

Five healthy volunteers, including myself, (three females, age:  $27 \pm 1$ ) participated in our study. They had normal or corrected-to-normal vision and no history of neurological or visual disorders. Participants were not diagnosed for any psychiatric disorder and they were not using any psychiatric drugs. All participants gave their written informed consents prior to each experimental sessions. Experimental protocols and procedures were approved by the Human Ethics Committee of Bilkent University.

### 2.2 Stimuli Presentation

For pRF mapping, drifting bars [6] are used as a novel stimulus [1, ?, 41]. However, Alvarez and his colleagues suggested to use rotating wedge presented simultaneously with expanding/contracting rings compared them and showed that the drifting bar stimulus required more experimental duration than simultaneous wedge and ring stimulus to construct maps with similar goodness-of-fit [27]. After

this study, simultaneous wedge and ring stimulus are used for many pRF studies [42, 30]. Therefore, both stimulus types are widely used for pRF estimations. We preferred to use simultaneous wedge and ring stimulus because of time concern by having three different conditions making the experiment three-times longer.

We had three different types of images rendered into the simultaneous wedge and ring mask: scrambled, neutral and emotional images. The scrambled images were the scrambled form of emotional ones. We divided each image into 30 square-shaped block and then, we shuffled the positions of those blocks randomly to created our scrambled images. Neutral and emotional images were selected from Nencki Affective Picture Set (NAPS) with respect to emotional ratings characterized by Riegel and her colleagues [43]. This rating system defined six emotional categories: happiness, sadness, fear, surprised, anger and disgust. 24 images defined as fear-triggering were used in emotional condition. The fearful images included wild animals such as growling dog or snakes and a soldier pointing a gun. We selected the images which were rated below average for each type of emotions as neutral images. As a result, we had 59 neutral images. The neutral images included tropical trees, faces, buildings and objects such as a bicycle and kitchen tools. Since we presented a small part of images at each step, it can be argued that the content of image could not be perceived by participants. However, Zuiderbaan, Harvey and Dumoulin showed that the images rendered into pRF stimuli could be decoded by using machine-learning algorithm [44]. This proves the participants can perceive the presented part of the image at each step, which is enough to trigger target emotional state.

The experiment was divided into three fMRI sessions in which participants were presented the simultaneous wedge and ring stimuli rendered with scrambled images, neutral images and emotional images; respectively. (see Figure 2.1 as a representation of presented stimuli) Since Jelle A. van Dijk and his colleagues (2016) showed that the pRF estimations were reliable among different sessions [42], we could compare the results coming from different sessions.

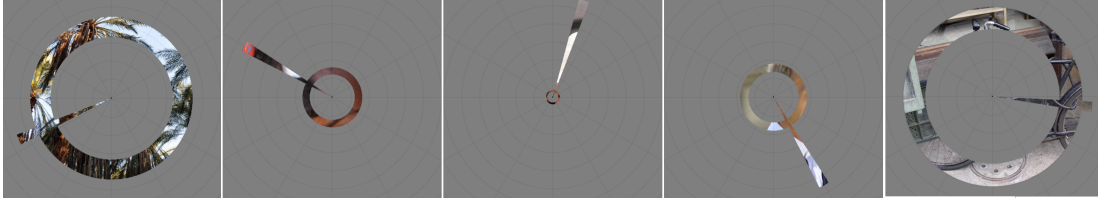


Figure 2.1: **Representation of stimulus in the experiment.** The representative figures show the stimuli presented during the experiment. The images here are some of the neutral images. In the background, there is a low-contrast spiderweb.

## 2.3 Experimental Protocol and MR Image Acquisition

pRF mapping stimuli were the simultaneous wedge and ring rendered with images. In each session, the order of images was randomized per run, and a new image was presented every 500 ms. An fMRI session includes 12 scans by repeating two different motion of stimuli. During the odd runs, the wedge ( $6^\circ$  angle) rotated counter-clockwise for 3 cycles (60 steps per cycle) and the ring expanded for 5 cycles (36 steps per cycle) whereas during the even runs the wedge rotated clockwise and the ring contracted with the same parameters. (see Figure 2.2) Each step was presented for the duration of one TR (2 s). The maximum radius of ring and the length of wedge was 6.75 visual degree. The diameter of the outer boundary, for the ring, was determined by the following scaling function:

$$f(x) = (\text{maxDiameter}) * e^{(-4+x/9)}$$

where *maxDiameter* was 13.5 visual degree in our experimental set-up and  $x$  was either increasing or decreasing at each step of cycle in integer steps from 1 to 36 for expanding or contracting ring, respectively. The radius of the inner boundary of ring was 75% of the radius of the outer boundary at the minimum eccentricity. Otherwise, it is 25% of the radius of outer boundary. We presented the stimuli on a gray background with a luminance 65.5648 cd / m<sup>2</sup>.

To ensure fixation, a low-contrast spider web was drawn at the gray background. Additionally, participants were asked to perform a fixation task in which

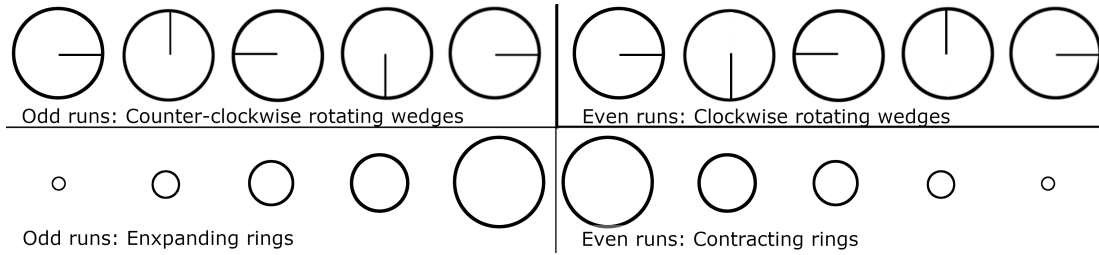


Figure 2.2: **Order of stimulus in the experiment.** The representative figures shows the order of positions of the stimuli during the experiment. In odd runs, we presented expanding rings and counter-clockwise rotating wedges simultaneously. In even runs, contracting rings and clockwise rotating wedges were presented simultaneously. One run included 3 cycles of wedges and 5 cycles of rings. One cycle of wedges had 60 steps whereas one cycle of rings had 36 steps.

the color of fixation point (0.13 visual degree solid circle) changed randomly into either red or green from its original color, black. The fixation task was for a duration of 200 ms with a probability 0.1. The participants were asked to report the color change by pressing the designated button on an MR-safe response button-box (Fiber Optic Response Devices Package 904, Current Designs). To separate the fixation point from the stimuli, a ring-shaped mask colored as background color (gray) was placed around the fixation point with a outer boundary of 0.26 visual degree.

Stimuli were projected on an MR-safe LCD screen (1920px X 1080px resolution, dimensions 125 cm x 70 cm, vertical refresh: 60 Hz, TELEMED PMEco, İstanbul) at the back of the scanner bore and viewed via a mirror on the head coil. The resulting total viewing distance was 165 cm. All stimuli were generated using MATLAB R21016b and PsychToolBox [45].

MR data were collected on a 3 Tesla Siemens Trio scanner (Magnetom Trio, Siemens AG, Erlangen, Germany) by using 32-channel head coil in National Magnetic Resonance Research Center (UMRAM), Bilkent University. Each MR session started with a short localizer to check the location of head. It was followed by a structural scan, and 12 functional scans in each session. The structural data were acquired by using a T1-weighted 3-D anatomical scan (TR: 2600 ms, spatial resolution: 1 mm<sup>3</sup> isotropic, number of slices: 176). The functional images were

acquired with a T2\*-weighted gradient-recalled multi-band echo-planar imaging (EPI) sequence (TR: 2000 ms, TE: 60 ms, spatial resolution: 1.6x1.6x1.6 mm<sup>3</sup>, number of slices: 84, multi-band acceleration factor: 6, slice orientation: parallel to calcarine sulcus). Duration of each session was approximately one and a half hour.

## 2.4 Analysis

### 2.4.1 Preprocessing of MR Data

For structural preprocessing, FreeSurfer version 6.0.0 was used. Reconstruction function *recon-all* was used for structural preprocessing [46, 47, 48, 49, 50, 51, 52, 53]. The steps that *recon-all* apply are the following: (1) Motion correction, (2) Intensity correction, (3) Talairach transformation, (4) Normalization, (5) Skull strip, (6) Automatic subcortical segmentation, (7) Automatic segmentation statistics, (8) White matter segmentation, (9) Cut/Fill to separate two hemisphere in the corpus callosum, (10) Surface smoothing, (11) Inflation, (12) Automatic topology fixer, (13) Final surfaces of white matter, pial and cortical thickness, (14) Cortical ribbon mask, (15) Spherical inflation, (16) Surface registration to ipsilateral and contraletal atlas, (17) Average curvature, (18) Cortical parcellation, (19) Parcellation statistics.

Then, we coregistered the structural images of emotional and neutral conditions for each subject onto the structural image of scrambled condition. Hence, we could average the structural images by using SPM image calculation tool. We preprocessed the averaged structural image by using FreeSurfer function *recon-all*.

For functional preprocessing, we used SPM12 [54]. Since the data format of our scanner was a type of DICOM, we started the preprocessing with importing DICOM. The following steps were realign and unwarp of functional data followed by coregistration of functional data with structural images. Then, we performed a second coregistration of the structural preprocessed image of that condition to the

averaged structural image. We used the same coregistration matrix to coregister the functional data of that condition onto the averaged structural preprocessed image. We performed those steps for every conditions of each subject.

Then, we merged our 3D data into 4D NII files since the following steps would require 4D NII files. We averaged the odd numbered runs (in which expanding ring and counter-clockwise rotating wedge were presented) and even numbered runs (in which shrinking ring and clockwise rotating wedge were presented) separately. We merged the averaged data, and the final functional data file included averaged data for expanding ring and counter-clockwise rotating followed by averaged data for shrinking ring and clockwise rotating wedge. We projected the final functional data onto the averaged structural preprocessed image. After this projection, the voxels of functional data were interpolated to the resolution of structural images which was 1 mm x 1 mm x 1 mm. Therefore, we had vertices instead of voxels. Since we used the data corrected for head motion from the scanner, we did not apply a second motion correction in preprocessing.

### **2.4.2 Analysis of the Response to Fixation Task**

We collected the response of participants to the fixation task. The data included which color the participant reported by pressing one of the two buttons (color response) and when the participant pressed the button (response time). We calculated the ratios of correct answers in each run for each subject. Then, we averaged the correct ratios for each condition. Similarly, we calculated the time delay in response of subjects in each run. Then, we averaged the time delay in each condition for each subject. We performed a one-way ANOVA for the correct ratios for scrambled, neutral and emotional conditions. As well, we performed a one-way ANOVA for the time delay for scrambled, neutral and emotional conditions.



### 2.4.3 pRF Estimation

For pRF model fit, we used SamSrf toolbox created by Samuel Schwarzkopf's lab [55]. The model used for the fit was an isotropic 2D Gaussian function. The output of pRF model fit includes  $R^2$ ,  $X_0$ ,  $Y_0$ , sigma, beta, baseline, field sign, CMF (cortical magnification factor) and visual area.  $R^2$  means the reliability of the estimations.  $X_0$  and  $Y_0$  are the coordinates of each estimated receptive field on visual field. Sigma is the standard deviation from its mean of the Gaussian curve of each pRF. In other words, sigma is tightly related to the pRF size. Beta is the amplitude of averaged BOLD response in each vertex. Baseline is the amplitude of baseline activation derived from the non-stimulated areas or from the background. It is computed by z-standardizing the BOLD data in inactive vertices. Field sign indicates whether or not the vertex represents the mirror image of the stimulus. As we mentioned in Chapter 1, some retinotopic regions represent the stimulus as nonmirror such as V1. If the representation is nonmirror (i.e., the activation travels from dorsal side to ventral side on one hemisphere while a wedge rotates clockwise on the corresponding visual hemifield), the field sign for the corresponding vertices is 1 in pRF estimations. On the other hand, if the cortical area such as V2v represents the stimulus as mirror (i.e., the activation travels from ventral side to dorsal side while a wedge rotates clockwise), the field signs of the vertices are estimated as -1. For the vertices which cannot be defined as retinotopic region, the field sign is estimated as 0. CMF is a calculated value using other estimations. It indicates how much the represented visual area is magnified on the cortex. Since they are calculated after smoothing the data, field sign and CMF values are not so reliable as the other outputs. Visual area includes the information about estimated locations of retinotopic regions for each vertex after smoothing. Additionally, we have the information about number of vertices in which the model fit is performed. Using those outputs, we can use SamSrf toolbox for delineation of retinotopic regions and to visualize the maps. We used the estimations for emotional condition for delineation using the estimated polar, eccentricity and field sign maps. Those delineations fitted to neutral and scrambled conditions since the retinotopic organization did not change due to the stimulus content.

We used sigma values,  $X_0$ ,  $Y_0$  and number of vertices among the outputs of pRF estimation for further analysis. To extract data from the SamSrf output, we selected the vertices having a reliability value bigger than 0.05 and corresponding to an eccentricity range from 0.5 to 6.75 since the estimations for an eccentricity below 0.5 can have lower reliability and the estimations for an eccentricity above 6.75 would be error considering our stimulus size (maximum radius was 6.75). We extracted the pRF size and location ( $X_0$  and  $Y_0$ ) estimations at the selected vertices. Then, we calculated the eccentricity of pRF center by using  $X_0$  and  $Y_0$  values with the following formula:

$$eccentricity\_pRFcenter = \sqrt{X_0^2 + Y_0^2}$$

Additionally, we calculated the polar angle of each location of pRF center by using  $X_0$  and  $Y_0$  values with the following formula:

$$polarAngle\_pRFcenter = \tan^{-1}(X_0, Y_0)$$

For statistical analysis, we used MATLAB R2016b. First, we performed paired t-test between the number of reliable vertices for emotional and scrambled conditions to check the effect of scrambling on the size of map compared to a coherent image. Second, we performed repeated measures ANOVA with repeated measures factors of sigma values estimated at the common reliable vertices of every subjects for emotional and scrambled conditions and with repeated measures factors of the locations of pRF centers for emotional and scrambled conditions to understand the effect of scrambling compared to a coherent image. The between subject factors were individual subjects and hemispheres. Third, we compared the beta values, which are the BOLD amplitudes in the common reliable vertices, across emotional and scrambled conditions by performing a paired t-test. Then, we compared the number of reliable vertices for emotional and neutral conditions via additional paired t-test. If there would be no significant difference between the sizes of maps constructed in emotional and neutral conditions whereas there is a significant difference between the sizes of maps constructed for emotional and scrambled conditions, it would support that the coherence of the images in the stimulus content might affect the size of map constructed using pRF estimations.

Afterwards, we compared the sigma values at common reliable vertices for emotional and neutral conditions via repeated measures ANOVA with repeated measures factors of the locations of pRF centers for emotional and neutral conditions to understand the effect of the stimulus with emotional content. The between subject factors were individual subjects and hemispheres. Finally, we compared the beta values, which are the BOLD amplitudes in the common reliable vertices, for emotional and neutral conditions by performing a paired t-test.

#### **2.4.4 Analysis of Image Properties**

We analyzed the images that we used in the current study in terms of saliency. We used MATLAB source code for Graph-Based Visual Saliency [56] and created saliency maps of images. Then, we averaged the maps to compare three conditions in terms of the averaged salient locations on the images.

# Chapter 3

## Results

### 3.1 The Effect of Image Coherence

We compared the results of emotional and scrambled conditions to check the effect of meaningful, coherent image on pRF estimation. The emotional and scrambled images had the same low-level features such as brightness and contrast. Therefore, the comparison between emotional and scrambled conditions would be the comparison between meaningful, coherent content and scrambled version which was appeared like combined colored squares.

#### 3.1.1 The Size of Maps

Firstly, the map estimated for emotional condition was wider than the map estimated for scrambled condition, which means that more area on visual cortex could be reliably estimated for emotional condition than for scrambled condition. It can be observed visually on Figure 3.1. To compare the vertex number which the maps constructed for scrambled and emotional conditions, we extracted the number of reliable vertices for both conditions of each subject. We used SamSrf plot function to find the number of vertices with a reliability more than 0.05. The

Table 3.1: Number of reliable vertices on each hemisphere of each subject in emotional and scrambled conditions

	Left hemisphere		Right hemisphere	
	Emotional	Scrambled	Emotional	Scrambled
Subject 1	8225	5783	8550	5775
Subject 2	8411	6984	11135	7859
Subject 3	8093	6948	8314	7021
Subject 4	6292	5041	7668	6504
Subject 5	5734	5498	7745	6771

data was shown in Table 3.1. The number of reliable vertices for scrambled condition were always smaller than the number of reliable vertices for emotional condition. Since the maps are constructed for left and right hemispheres separately, we performed paired t-test for left and right hemispheres as well as paired t-test for the overall data as comparisons between scrambled and emotional conditions. As a result of paired t-tests, the number of reliable vertices for scrambled condition were significantly smaller than the number of reliable vertices for emotional condition ( $t = -3.69$ ,  $p = 0.021$  for left hemisphere;  $t = -4.03$ ,  $p = 0.016$  for right hemisphere and  $t = -5.43$ ,  $p = 4.157 \times 10^{-4}$  for overall).

We can say that the maps of emotional condition was better to delineate than the maps of scrambled condition in terms of the number of reliably defined retinotopic regions. It was harder to define V4 and V3A on the maps constructed for scrambled condition than on the maps for emotional condition. Moreover, more region at dorsal side could have been defined in emotional condition. However, we did not delineate more regions for two reasons. First, we could not compare the data of emotional and scrambled conditions at those regions such as V3B since we would have almost no data in scrambled condition. Second, we focused on ventral stream since the emotional modulation was shown to affect ventral stream rather than dorsal stream [4, 5]. We can conclude that the coherent images resulted in better pRF maps than their scrambled versions. The difference can be visually observed between the maps of emotional and scrambled conditions consistently in each subject (see Appendix C).

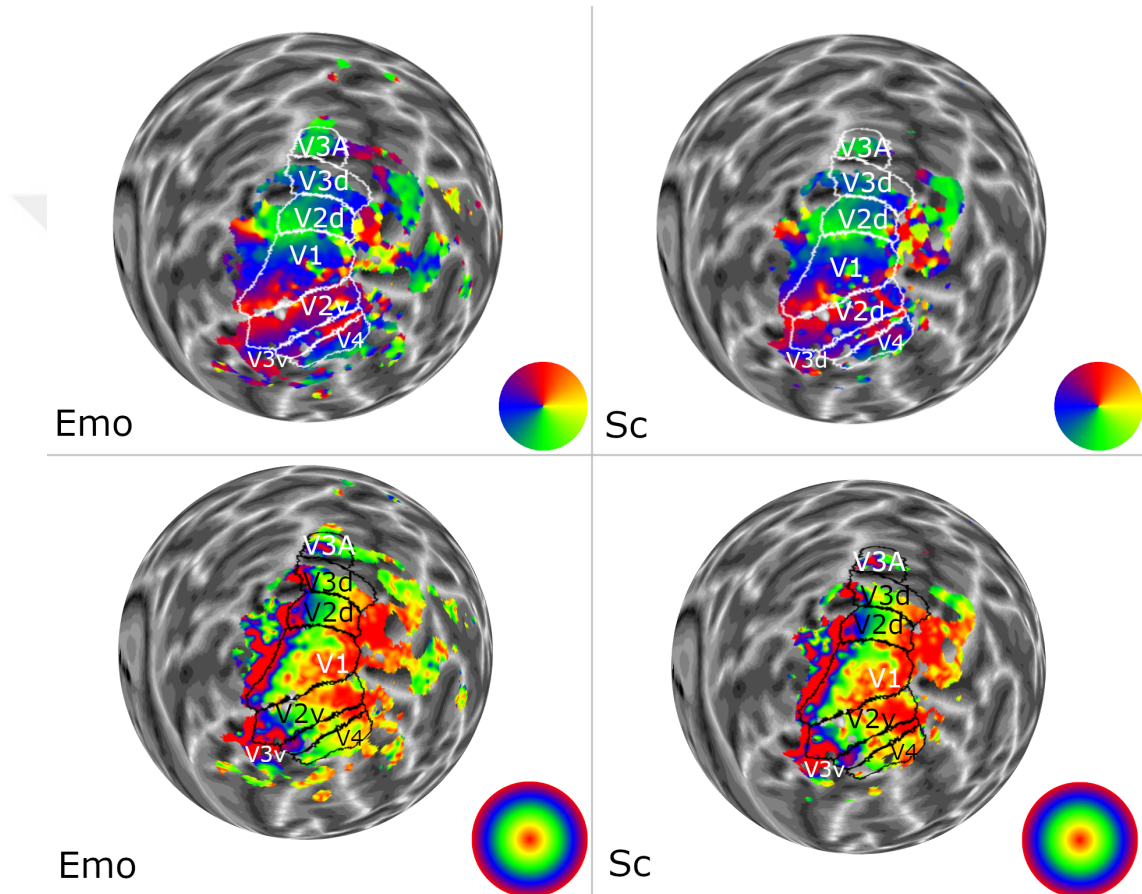


Figure 3.1: **Representative maps of emotional and scrambled conditions.** The right hemisphere of Subject 2 is shown. The images at the upper part of figure are polar maps whereas the images at the lower part of figure are eccentricity maps. The circular legend at the upper images indicates the corresponding colors for every polar angle. The circular legend at the lower images indicates the corresponding colors for every eccentricity. The retinotopic regions are labelled on the figure. “Emo” stands for emotional condition and “Sc” stands for scrambled condition on the figure. Retinotopic regions can be delineated better on the map constructed for emotional condition compared to the map constructed for scrambled condition.

### 3.1.2 The Change in pRF Estimations

Secondly, we analyzed the pRF sizes estimated for scrambled and emotional conditions. As we mentioned previously, the stimulus content can change pRF sizes [2, 1]. Therefore, we extracted the sigma values at vertices with reliable model-fit for scrambled and emotional conditions. Data included the estimated sigma values at the vertices with more than 0.05 reliability value and at a range of eccentricity from 0.5 to 6.75 visual degree. The mean pRF size in scrambled condition was 2.33 whereas the mean pRF size in emotional condition was 2.47. We compared the estimated sigma values for emotional and scrambled conditions by using repeated measures ANOVA (rmANOVA) with subjects and hemispheres as between-subject factors. The statistical results can be found in Table 3.2. The group analysis showed the emotional condition resulted in larger sigma values than their scrambled versions in occipital lobe, which means the content of stimuli can affect the pRF estimations. This finding was consistent across subjects. Moreover, we performed rmANOVA in each retinotopic regions between emotional and scrambled conditions. The results showed that there is a significant difference in pRF sizes in all the retinotopic regions that we could delineate (see Table 3.2). The descriptive plot of pRF sizes in scrambled and emotional conditions is shown on Figure 3.2. Moreover, we found a significant interaction between subjects and conditions in all ROIs (see Table 3.2). This indicates that there is an individual differences in the effect of coherent images and of their scrambled versions on the pRF size. Another between subjects factor was hemispheres. We found that there was a significant interaction between hemispheres and conditions in occipital lobe. When we analyzed the data in each retinotopic region, we found that the interaction between hemispheres and conditions was significant in V2v, V3d, V3v, V3A and V4 as shown in Table 3.2.

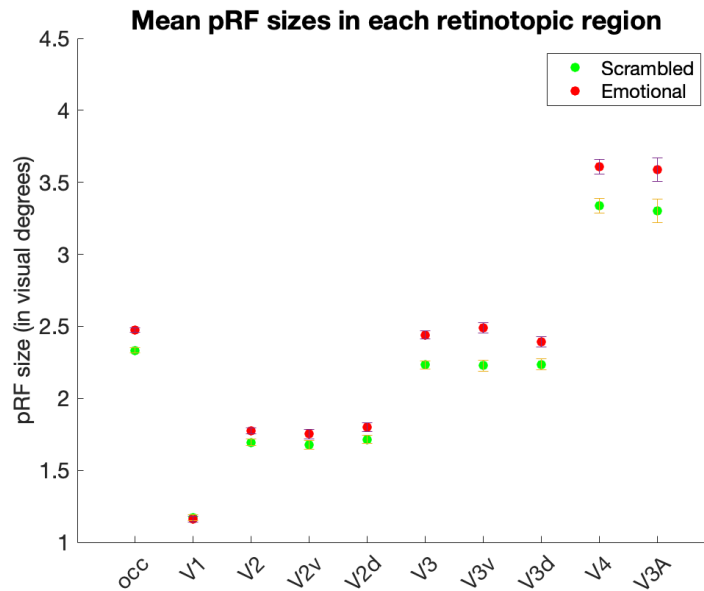


Figure 3.2: **Descriptive plot of pRF sizes estimated for scrambled and emotional conditions.** The points on the figure represent the mean of the estimated sigma values in each ROI. The red circles represent the emotional data and the green circles represent the scrambled data. The error bars indicate the 95% confidence interval.

We also compared the pRF locations since, as we mentioned previously in Chapter 1, Dongjun He and his colleagues showed that the location of pRF center might change due to the stimulus content although they did not analyse the pRF sizes in that study [3]. To compare the locations of pRF centers, we extracted the estimated  $X_0$  and  $Y_0$  values from the pRF fit results. Then, we calculated the location of pRF center as we mentioned in Chapter 2. We performed repeated measures ANOVA (rmANOVA) with the pRF center data of scrambled and emotional condition. The statistical results can be found in Table 3.3. We found that the pRF centers shift toward the more eccentric side in each retinotopic regions in emotional condition compared to scrambled condition (see Table 3.3). The mean locations of pRF centers in each ROI is shown in Figure 3.3. Additionally, there was a significant interaction between subjects and conditions in occipital lobe and each retinotopic region (see Table 3.3). This points to the individual differences in pRF shift. Moreover, the interaction between hemispheres and conditions was significant in V2v, V3v, V3A and V4 (see Table 3.3).



Table 3.2: The results of repeated measures ANOVA between the sigma values of scrambled and emotional condition

		F-value	p-value
occ	conditions	1165	0.019
	conditions X subjects	408	$1.79 \times 10^{-5}$
	conditions X hemispheres	181	0.047
V1	conditions	63841	0.002
	conditions X subjects	130	0.0002
	conditions X hemispheres	17	0.15
V2d	conditions	1715	0.015
	conditions X subjects	200	$7.40 \times 10^{-5}$
	conditions X hemispheres	8.3	0.21
V2v	conditions	2124	0.014
	conditions X subjects	76	0.0005
	conditions X hemispheres	223	0.043
V3d	conditions	874	0.022
	conditions X subjects	29	0.003
	conditions X hemispheres	298	0.037
V3v	conditions	324	0.035
	conditions X subjects	21	0.006
	conditions X hemispheres	296	0.037
V3A	conditions	577	0.026
	conditions X subjects	182	$8.90 \times 10^{-5}$
	conditions X hemispheres	11047	0.006
hV4	conditions	668	0.025
	conditions X subjects	58	0.0009
	conditions X hemispheres	354	0.034

*Note.* The “conditions” indicates the change in the sigma values between two conditions. The degree of freedom is 1 for “conditions” and it is 4 for the interactions with “subjects” and “hemispheres”.

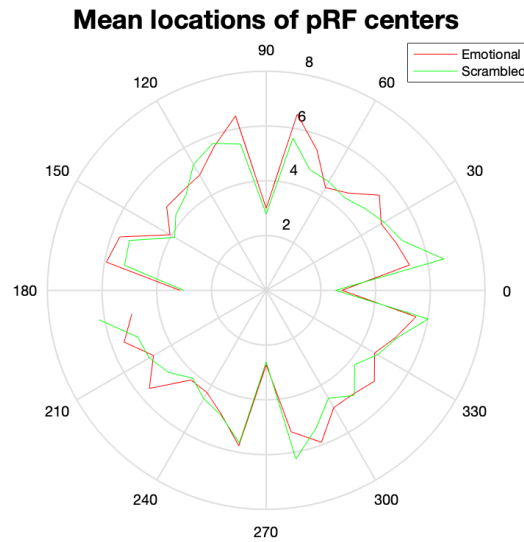


Figure 3.3: **Radial map of locations of pRF centers calculated for scrambled and emotional conditions.** The locations of pRF centers were calculated by using the estimated  $X_0$  and  $Y_0$  values at the reliable vertices in scrambled and emotional condition. The lines on the figure represent the mean of the calculated values for the locations of pRF centers in occipital lobe at each polar coordinate of visual field. The red line represents the emotional data and the green line represents the scrambled data. As shown on the figure, the pRF centers in scrambled condition were located at lower eccentricity compared to emotional condition. In other words, the pRF centers in scrambled condition were closer to fovea than the pRF centers in emotional condition.

These results indicated the difference in the response level of left and right hemisphere to emotional and scrambled conditions.

We compared the amplitude of BOLD activity in emotional and scrambled conditions since Rainer and his colleagues showed the natural images might lead to increased BOLD in visual cortex activity compared to noise pattern [57]. We extracted the beta values which are the amplitude of BOLD signal in each vertex having a reliability value bigger than 0.05 and at a range of eccentricity from 0.5 to 6.75. We compared the data with t-test. We found the amplitude of BOLD signal is larger in emotional condition compared to scrambled condition in V1, V3d, V3v, V3A and V4 (see Table3.4).

Table 3.3: The results of repeated measures ANOVA between the pRF centers of scrambled and emotional condition

		F-value	p-value
occ	conditions	2028	0.014
	conditions X subjects	122	0.0002
	conditions X hemispheres	23	0.13
V1	conditions	8060	0.007
	conditions X subjects	81	0.0004
	conditions X hemispheres	65	0.08
V2d	conditions	1787	0.015
	conditions X subjects	203	$7.18 \times 10^{-5}$
	conditions X hemispheres	2.5	0.36
V2v	conditions	1368	0.017
	conditions X subjects	246	$4.92 \times 10^{-5}$
	conditions X hemispheres	3760	0.011
V3d	conditions	996	0.020
	conditions X subjects	90	0.0003
	conditions X hemispheres	153	0.051
V3v	conditions	415	0.0312
	conditions X subjects	158	0.0001
	conditions X hemispheres	476	0.029
V3A	conditions	1527	0.016
	conditions X subjects	69	0.0006
	conditions X hemispheres	197	0.045
hV4	conditions	843	0.022
	conditions X subjects	51	0.001
	conditions X hemispheres	2422	0.013

*Note.* The “conditions” indicates the change in the locations of pRF centers between two conditions. The degree of freedom is 1 for “conditions” and it is 4 for the interactions with “subjects” and “hemispheres”.

Table 3.4: The results of t-test between the beta values of scrambled and emotional condition

	df	t-value	p-value
occ	28290	-18.0	< 0.05
V1	6540	8.20	$3.3 \times 10^{-16}$
V2d	2531	1.20	0.23
V2v	3014	1.08	0.28
V3d	2484	-2.47	0.014
V3v	2435	-3.31	0.00094
V3A	1892	-6.48	$1.8 \times 10^{-10}$
hV4	646	-14.07	< 0.05

## 3.2 The Effect of Emotion

We compared the results of emotional and neutral conditions to investigate the effect of emotion on sigma values. Since both conditions included coherent meaningful images, the difference in results indicates the effect of triggered emotion.

### 3.2.1 The Size of Maps

The size of maps constructed for emotional and neutral conditions were visually similar. Nevertheless, we performed paired t-test between the number of reliable vertices for emotional and neutral conditions. We extracted the number of reliable vertices by using SamSrf plot function for both conditions of each subject. As shown in Table 3.5, the numbers of reliable vertices for emotional and neutral condition are very close. As we did for the comparison between scrambled and emotional conditions, we analyzed the data for left and right hemispheres separately since the maps were separately constructed for two hemispheres. We compared the overall data as well. As a result of paired t-tests, the number of reliable vertices in emotional and neutral conditions were very close. The number of reliable vertices was not significantly different in two conditions ( $t = 0.91$ ,  $p = 0.91$  for left hemisphere;  $t = 1.19$ ,  $p = 0.30$  for right hemisphere and  $t = 0.52$ ,  $p$

= 0.52 for overall). Moreover, we could define almost same regions in emotional and neutral conditions as shown in representative map on Figure 3.4.

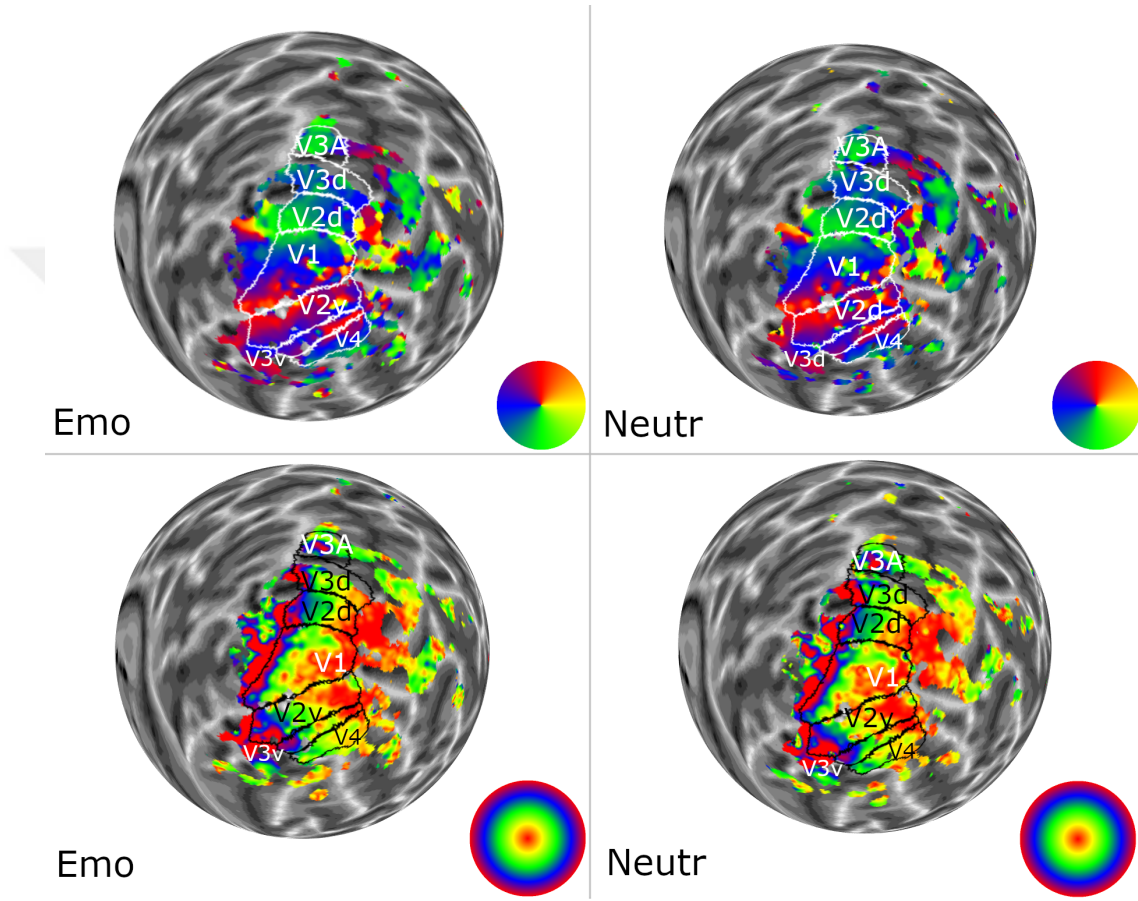


Figure 3.4: **Representative maps of emotional and neutral conditions.** The right hemisphere of Subject 2 is shown. The images at the upper part of figure are polar maps whereas the images at the lower part of figure are eccentricity maps. The circular legend at the upper images indicates the corresponding colors for every polar angle. The circular legend at the lower images indicates the corresponding colors for every eccentricity. The retinotopic regions are labelled on the figure. The maps constructed for emotional and neutral conditions are very similar to each other.

Table 3.5: Number of reliable vertices on each hemisphere of each subject in emotional and neutral conditions

	Left hemisphere		Right hemisphere	
	Emotional	Neutral	Emotional	Neutral
Subject 1	8225	7210	8550	8296
Subject 2	8411	8602	11135	11490
Subject 3	8093	7332	8314	8765
Subject 4	6292	6979	7668	9026
Subject 5	5734	6425	7745	7555

### 3.2.2 The Change in pRF Estimations

We compared the pRF sizes and locations estimated for emotional and neutral conditions to understand how emotional modulation can affect the process in visual cortex. For the comparison, we selected the reliable vertices to extract data with a threshold of 0.05 for reliability value. As a result, we extracted sigma,  $X_0$  and  $Y_0$  values at the vertices which corresponds to a range of eccentricities from 0.5 to 6.75. Then, we calculated the locations of pRF centers for both conditions as described in Chapter 2.

In our data, the mean pRF size in emotional condition was 2.90 whereas the mean pRF size in neutral condition was 2.85. Then, we performed repeated measures ANOVA between the locations of pRF centers for neutral and emotional conditions in occipital lobe and in each retinotopic region that we delineated with between subjects factors of individual subjects and hemispheres. The statistical results can be found in Table 3.6. The pRF sizes in emotional condition were significantly larger than the pRF sizes in neutral condition. The increase in pRF size in emotional condition was significant in occipital lobe and each retinotopic region (see Table 3.6). The change in pRF sizes is shown visually on Figure 3.5. Moreover, there is a significant interaction between subjects and conditions (see Table 3.6), meaning that the level of emotional modulation differs among the individuals. Moreover, there is a significant interaction between hemispheres and conditions in occipital lobe (see Table 3.6). Therefore, we can say that there is a hemispheric asymmetry in emotional modulation. When we analyzed each retinotopic region, we found that the hemispheric asymmetry is significant only

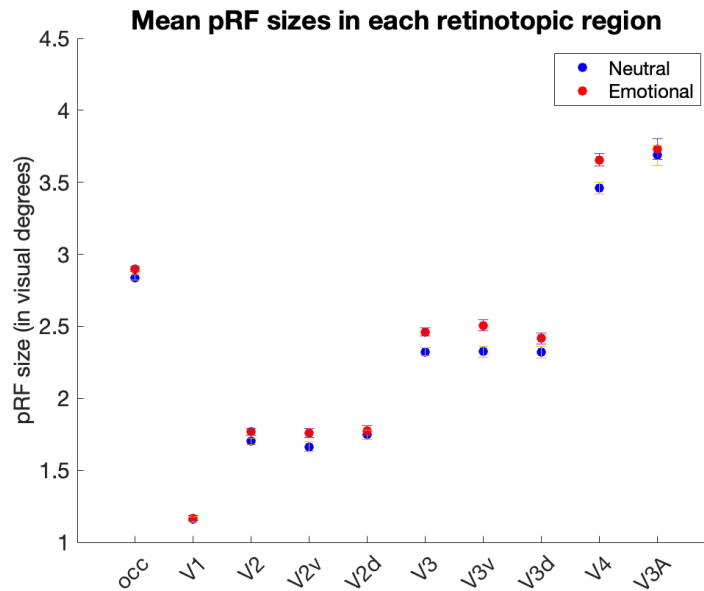


Figure 3.5: **pRF sizes estimated for neutral and emotional conditions.** The points on the figure represent the mean of the estimated sigma values in each ROI. The red circles represent the emotional data and the blue circles represent the neutral data. The error bars indicate the 95% confidence interval.

in V1, V2v, V3A and V4 (see Table 3.6).

We also analyzed whether there was a shift in pRF centers by performing repeated measures ANOVA between the calculated data of locations of pRF centers in emotional and neutral conditions. The statistical results can be found in Table 3.7. We found that the pRF centers shifted towards the eccentric side in emotional condition compared to neutral condition significantly at each ROI except V3A (see Table 3.7). The change in the locations of pRF centers was shown visually in Figure 3.6. The individual differences in emotional modulation was also found in the location of pRF centers. The interaction between subjects and conditions was significant in all ROIs (see Table 3.7). Moreover, the asymmetry between hemispheres significantly affected also the emotional modulation of pRF centers in occipital lobe (see Table 3.7). The interaction between hemispheres and conditions was significant in V2v, V3A and V4 (see Table 3.7).

Table 3.6: The results of repeated measures ANOVA between the sigma values of neutral and emotional condition

		F-value	p-value
occ	conditions	9301	0.0066
	conditions X subjects	3479	$2.48 \times 10^{-7}$
	conditions X hemispheres	1076	0.019
V1	conditions	56326	0.0027
	conditions X subjects	132	0.00017
	conditions X hemispheres	292	0.037
V2d	conditions	15362	0.0051
	conditions X subjects	66	0.00067
	conditions X hemispheres	0.7	0.56
V2v	conditions	1273	0.018
	conditions X subjects	763	$5.13 \times 10^{-6}$
	conditions X hemispheres	461	0.030
V3d	conditions	2421	0.013
	conditions X subjects	401	$1.86 \times 10^{-5}$
	conditions X hemispheres	25	0.13
V3v	conditions	700	0.024
	conditions X subjects	310	$3.09 \times 10^{-5}$
	conditions X hemispheres	2.2	0.38
V3A	conditions	29159	0.004
	conditions X subjects	284	$3.69 \times 10^{-5}$
	conditions X hemispheres	2741	0.012
hV4	conditions	1323	0.017
	conditions X subjects	24	0.0046
	conditions X hemispheres	1723	0.015

*Note.* The “conditions” indicates the change in the sigma values between two conditions. The degree of freedom is 1 for “conditions” and it is 4 for the interactions with “subjects” and “hemispheres”.



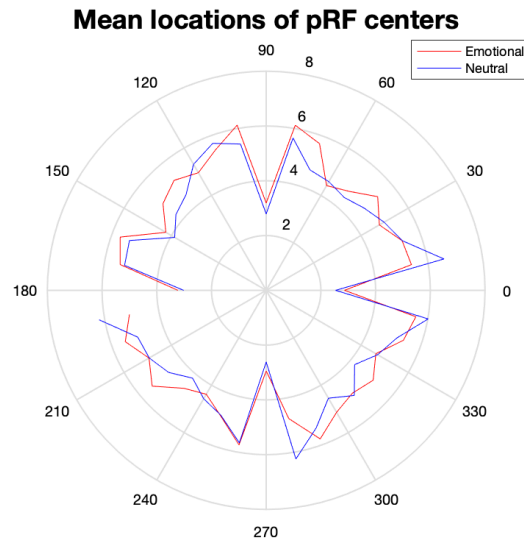


Figure 3.6: **Radial map of pRF centers calculated for neutral and emotional conditions.** The locations of pRF centers were calculated by using the estimated  $X_0$  and  $Y_0$  values at the reliable vertices in neutral and emotional condition. The lines on the figure represent the mean of the calculated values for the locations of pRF centers in occipital lobe at each polar coordinate of visual field. The red line represents the emotional data and the blue line represents the neutral data. As shown on the figure, the pRF centers in neutral condition were located at lower eccentricity compared to emotional condition. In other words, the pRF centers in neutral condition were closer to fovea than the pRF centers in emotional condition.

We compared the amplitude of BOLD activity in emotional and neutral conditions since it was shown that the BOLD activity might increase in emotional condition compared to neutral condition [4], and the increased BOLD activity can be related to the increase in pRF sizes in emotional condition compared to neutral condition. We used the data at the reliable vertices with a reliability value bigger than 0.05 and corresponding the eccentricity level from 0.5 to 6.75. We compared the data of emotional and neutral conditions by performing paired t-test. As a result, the amplitude of BOLD activity for emotional condition was significantly larger than the amplitude of BOLD activity for neutral condition in V2v, V3d, V3v and V4 (see Table 3.8).

Table 3.7: The results of repeated measures ANOVA between the pRF centers of neutral and emotional condition

		F-value	p-value
occ	conditions	3000	0.012
	conditions X subjects	519	$1.11 \times 10^{-5}$
	conditions X hemispheres	77370	0.0023
V1	conditions	1612	0.016
	conditions X subjects	103	0.00027
	conditions X hemispheres	90	0.067
V2d	conditions	2190	0.014
	conditions X subjects	334	$2.66 \times 10^{-5}$
	conditions X hemispheres	14	0.166
V2v	conditions	1405	0.017
	conditions X subjects	422	$1.67 \times 10^{-5}$
	conditions X hemispheres	2690	0.012
V3d	conditions	2779	0.012
	conditions X subjects	397	$1.89 \times 10^{-5}$
	conditions X hemispheres	59	0.082
V3v	conditions	1058	0.20
	conditions X subjects	22	0.0053
	conditions X hemispheres	2.6	0.353
V3A	conditions	173991	0.002
	conditions X subjects	72	0.00056
	conditions X hemispheres	225	0.042
hV4	conditions	1834	0.015
	conditions X subjects	12	0.018
	conditions X hemispheres	3966	0.010

*Note.* The “conditions” indicates the change in the locations of pRF centers between two conditions. The degree of freedom is 1 for “conditions” and it is 4 for the interactions with “subjects” and “hemispheres”.

Table 3.8: The results of t-test between the beta values of neutral and emotional condition

	df	t-value	p-value
occ	35401	-3.95	$7.8 \times 10^{-5}$
V1	6251	0.16	0.87
V2d	2412	0.23	0.82
V2v	2872	-5.20	$2.1 \times 10^{-7}$
V3d	2529	-3.87	0.00011
V3v	2463	-3.93	$7.9 \times 10^{-5}$
V3A	760	1.22	0.22
hV4	2405	-4.29	$1.9 \times 10^{-5}$

### 3.3 Fixation Task

During the experiment, the participants performed a fixation task. The color of fixation point changed its color randomly from its original color (black) either to red or to green for a duration of 200ms with a probability of 0.1. We analyzed the response of the participants to the fixation task for the comparison for any attentional differences between the conditions as described in Chapter 2. The averaged correct ratios of subjects can be found in Table 3.9. Moreover, the averaged time delay of each subject was presented in Table 3.10. In each run, participants were successful to identify the color of fixation point with an acceptable delay. The delay in response was not significantly different between the conditions ( $p = 0.51$ ,  $F = 0.7$ ,  $df = 2$ ). Additionally, the ratios of correct answers for the changed color was not significantly different between the conditions ( $p = 0.64$ ,  $0.47$ ,  $df = 2$ ). Hence, we can conclude that the difference in pRF estimations was not due to the difference in attention between the conditions. (for individual data, see Appendix C)

Table 3.9: The averaged ratios of correct answers for fixation task.

Subject	Scrambled	Neutral	Emotional
1	.9860	.9873	.9827
2	.9690	.9553	.9566
3	.9812	.9713	.9850
4	.9638	.9183	.8802
5	.9863	.9863	.9882

Table 3.10: The averaged time delay of response for fixation task.

Subject	Scrambled	Neutral	Emotional
1	.3722	.6166	.4522
2	.7293	1.5722	.6790
3	.4956	.3715	.4852
4	1.1083	6.3975	23.4284
5	.3944	.2931	.2838

### 3.4 Hemispheric Asymmetry

We compared the estimations for left and right hemisphere since we observed the effect of hemispheres in all conditions. We merged the data of each condition separately for left and right hemispheres. We rearranged our data of pRF size and the data of pRF center separately in each ROI. Then, we performed t-test for pRF size and for pRF center between two hemispheres. The pRF sizes estimated for right hemisphere was significantly larger than the pRFs sizes on left hemisphere ( $p < 0.05$ ). The larger pRF sizes in right hemisphere was significant in V1, V2d, V3d, V4 and V3A ( $p[V1] = 2.7 \times 10^{-9}$ ,  $p[V2d] = 0.00069$ ,  $p[V2v] = 0.93$ ,  $p[V3d] < 0.05$ ,  $p[V3v] = 0.36$ ,  $p[V3A] = 3.0 \times 10^{-11}$ ,  $p[V4] = 0.00077$ ). The difference in pRF sizes between two hemisphere is shown in Figure 3.7. When we analyze the pRF center data, we found no significant difference in locations of pRF centers for left and right hemispheres in occipital lobe ( $p = 0.67$ ). However, there was a significant difference between the locations of pRF centers in V1, V2d, V2v, V3d, V3A and V4 ( $p[V1] = 6.5 \times 10^{-5}$ ,  $p[V2d] = 0.0042$ ,  $p[V2v] = 0.011$ ,  $p[V3d] = 6.4 \times 10^{-12}$ ,  $p[V3v] = 0.86$ ,  $p[V3A] = 0.028$ ,  $p[V4] < 0.05$ ). In V1, V2v and V3d, the pRF centers shifted towards the fovea in left hemisphere as shown in Figure

3.8. On the other hand, the pRF centers of left hemisphere in V2d, V3A and V4 was at more eccentric side compared to the pRF centers of right hemisphere as shown in Figure 3.8.

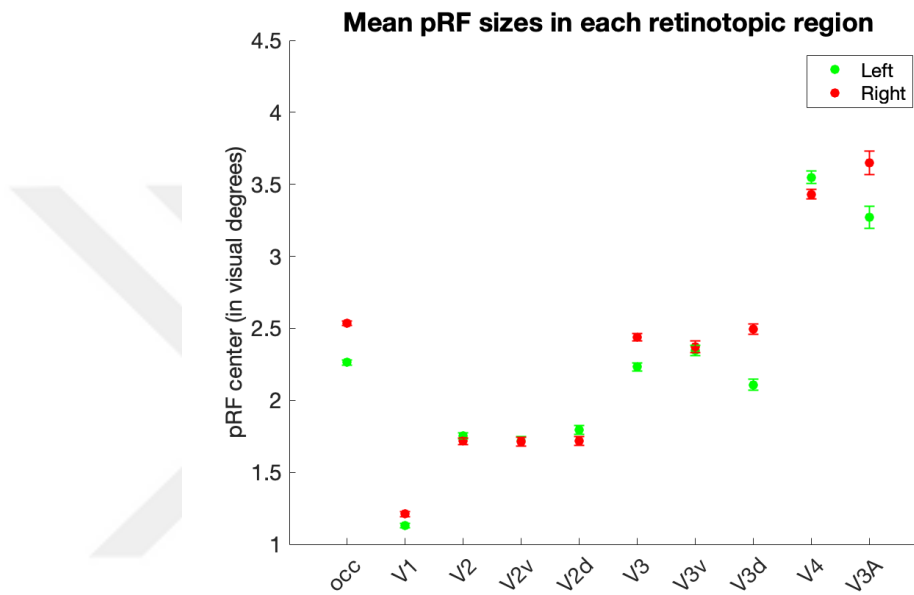


Figure 3.7: **Descriptive plot of pRF sizes on left and right hemispheres.** The error bars indicate 95% confidence intervals.

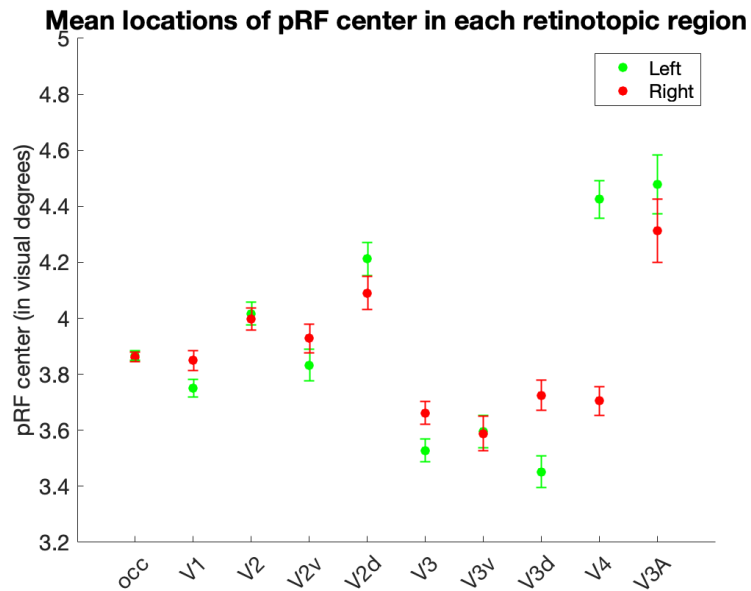


Figure 3.8: **Descriptive plot of the locations of pRF centers on left and right hemispheres.** The error bars indicate 95% confidence intervals.

### 3.5 Image Properties

We created saliency maps of each image to check if the shift in pRF centers was related with the difference in salient positions between the conditions. As shown in Figure 3.9, the salient positions of emotional and neutral images were very similar whereas the saliency was stronger at the central area of scrambled images. Therefore, we can say that the difference between the locations of pRF centers estimated for neutral and emotional condition is not related to the saliency whereas more salient central area of scrambled images might have a role in the shift in pRF centers towards the fovea. The pRF sizes located at the most salient points of images was not significantly different in each condition as shown in Figure 3.10. The saliency maps of each image can be found in Appendix B.

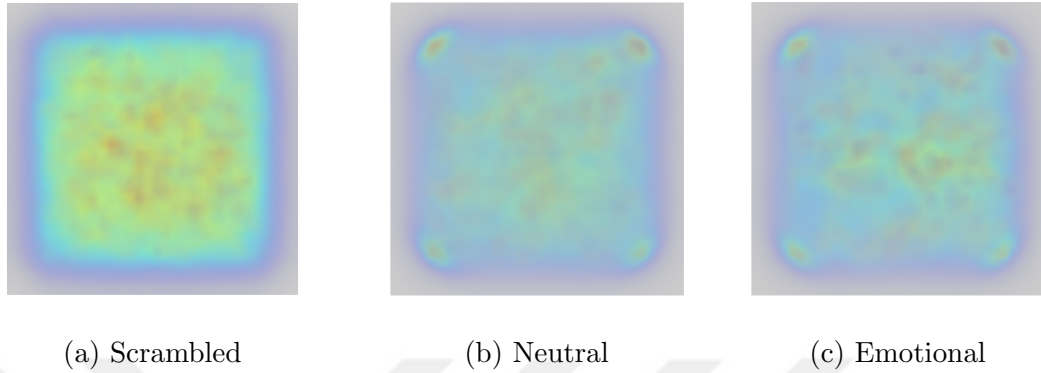


Figure 3.9: **The averaged saliency maps of conditions.** The saliency maps of images were created using Graph-Based Visual Saliency. Then, we averaged the saliency maps for each conditions. The saliency increases from blue to red color. (a) The averaged saliency map for scrambled images. (b) The averaged saliency map for neutral images. (c) The averaged saliency map for emotional images. As shown in the figure, the emotional images are very similar to neutral ones whereas the scrambled images have more salient points at the central area.

We compared luminance and contrast levels of scrambled, neutral and emotional conditions. We used the lookup table created using photometer to define the luminance value for each pixel of each image. Moreover, Michelson contrast was used to calculate the contrast of images. The averaged luminance in scrambled condition was  $63.5817 \text{ cd} / \text{m}^2$  and the averaged contrast value was 99.35%. The averaged luminance in neutral condition was  $67.9870 \text{ cd} / \text{m}^2$  and the averaged contrast value was 99.34%. The averaged luminance in emotional condition was  $64.0201 \text{ cd} / \text{m}^2$  and the averaged contrast value was 99.35%.

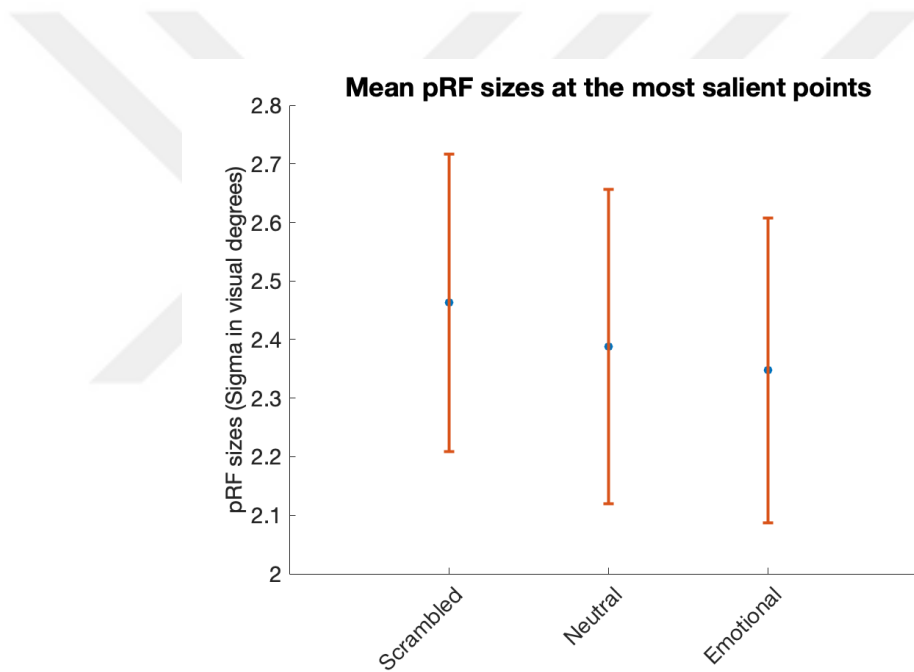
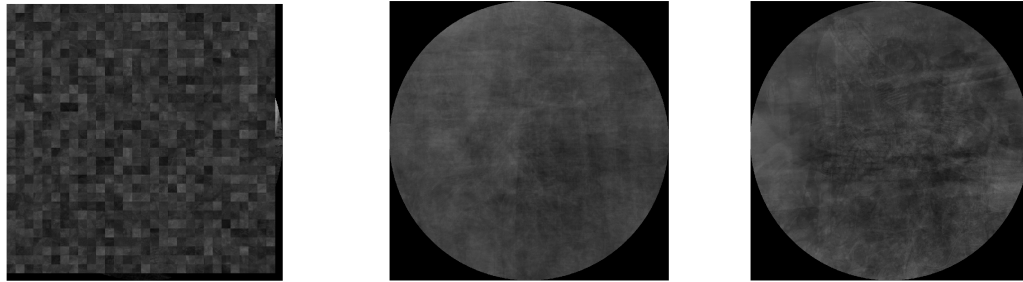


Figure 3.10: **The averaged pRF sizes at the most salient points for each condition.** The data points on the figure represent the averaged pRF size at the most salient points on the images presented during the session labelled on y-axis. The data were extracted from the reliable vertices common among three conditions. The error bars indicate 95% confidence interval.





(a) Scrambled  
mean lum: 63.5817 cd / m<sup>2</sup>  
mean contrast: 99.35%

(b) Neutral  
mean lum: 67.9870 cd / m<sup>2</sup>  
mean contrast: 99.34%

(c) Emotional  
mean lum: 64.0201 cd / m<sup>2</sup>  
mean contrast: 99.35%

Figure 3.11: **The averaged luminance of images in each condition.** Image (a) shows the luminance of scrambled condition in average. Image (b) shows the luminance of neutral condition in average. Image (c) shows the luminance of emotional condition in average. The averaged luminance and the averaged contrast values are shown for each condition on the figure.

# Chapter 4

## Discussion

In the current study, we investigated the effect of stimulus content on pRF estimations. The experimental design included two control conditions for emotional condition: one was scrambled condition and the other was neutral condition. The scrambled condition was a control of emotional condition to understand how the coherent images affect pRF estimation. Our second control was neutral condition to investigate the effect of negative emotion triggered by the visual stimuli. We showed that the content of stimulus can affect the population receptive field (pRF) estimations and the pRF parameters can be estimated better by using coherent images than using scrambled images. Moreover, our findings support the emotional modulation of the activity of visual cortex as shown in previous studies [4, 5]. The pRF size can be increased as a result of modulation of triggered emotion. Besides that, we showed that the effect of stimulus content was related to the individual differences. Finally, our findings support the idea of hemispheric asymmetry. We found the pRFs of right hemisphere were larger than the pRFs of left hemisphere under all stimulus conditions.

## 4.1 The coherent image is better for pRF mapping

Although natural scenes were used to analyze receptive fields mostly in electrophysiological studies [57, 58, 59], there are some vision researchers using natural scenes for the pRF estimation [42]. Direct comparison between coherent images and scrambled images was not found in the literature. Therefore, we compared the coherent images and their scrambled forms to check the power of coherent images.

By comparing the number of reliable vertices in emotional and scrambled conditions, we showed that the coherent images are better for pRF estimation than scrambled images. More vertices or wider area on the visual cortex can be mapped by using coherent images rather than scrambled images. As we mentioned previously, the functional ROI is important for neuroimaging studies. Therefore, mapping the wider area on cortex is an advantage of coherent images in pRF estimation method. Moreover, the increased number of reliable vertices in maps of emotional condition indicates that the pRF estimations in emotional condition is more reliable than the pRF estimations in scrambled condition. On the other hand, there was no significant difference in the size of maps in emotional and neutral conditions at which coherent images were presented. Hence, we can argue that using coherent images as stimulus of pRF estimation method is more advantageous than using a non-coherent stimulus such as scrambled images.

The estimated pRF sizes in emotional condition was larger than that in scrambled condition. The increased size in emotional condition could be due to the increased BOLD activity since it has been known that the natural images resulted in higher BOLD activity on brain than noise patterns [57]. We showed that the BOLD activity in emotional condition was significantly higher than the BOLD activity in scrambled conditions. Murray and his colleagues argued that the feedback mechanism from higher visual areas such as LOC could lead to the decreased in activity of lower visual areas such as V1 for the facilitation of object recognition [60]. Therefore, the increased pRF size in emotional condition can be

affected by increased BOLD activity for the facilitation of spatial processing of the stimulus. Moreover, we found that the pRF centers shifted towards the eccentric side in emotional condition compared to scrambled condition. The reason might be the difference in saliency between scrambled and emotional conditions. The central area of scrambled images were more salient than the peripheral area whereas the distribution of saliency for emotional image were more homogeneous than scrambled images. Hence, we can say that the pRF centers were shifted towards fovea in scrambled condition due to the more saliency at central area of scrambled images compared to the emotional condition.

## **4.2 Emotional content of stimulus might lead to an increased pRF size**

The stimulus with fearful images in our study led to an increased pRF size compared to the neutral condition. This effect was consistent in each retinotopic regions; V1, V2d, V2v, V3d, V3v, V3A and V4. On the other hand, previous findings related the ventral system to emotional modulation rather than dorsal stream [4, 5]. It has been also shown that the ventral stream (from V1 to TE) has direct projections from amygdala [39, 40]. However, our findings showed that the effect of stimulus with emotional cue might affect the pRF parameters in both ventral and dorsal stream. Therefore, the change in pRF parameters might be resulted from a feedback mechanism rather than direct projection from amygdala. Furthermore, no findings can be found in literature about the effect of fear on the retinotopic regions lower than hV4. We showed that the stimulus with emotional cue can affect the lower areas in visual system including V1, V2 and V3 as well as hV4 and V3A. Here, we argue that the emotional modulation as a feedback mechanism might lead to increased pRF sizes in visual cortex under fearful condition.

Previous fMRI studies showed an increased BOLD response on temporo-occipital side when the participants were triggered by positive or negative emotions [4]. We also found a significant increase in the amplitude of BOLD responses of emotional condition compared to scrambled and neutral conditions. Therefore, we can argue that the pRF sizes increase in response to visual stimuli with emotional cues, the increased information flow resulted from the increased pRF size can explain the increased BOLD activation.

The next question is whether the increased pRF size might lead to the facilitation or interruption of visual processing. Since it was argued that the emotional and attentional modulations were different mechanism but they used concurrent pathways [5, 33], the findings for attentional modulation on the visual process can be important to conclude emotional modulation.

Kendrick N. Kay and his colleagues investigated the pRF sizes in retinotopic regions in response to the attention by using face stimuli with a control condition of scrambled face [61]. The participants attended either the fixation dot or the face stimuli (or scrambled stimuli in control condition) presented at periphery. During those task, they measured pRF sizes in previously defined retinotopic regions by using a model they created. They found increase in pRF sizes in ventral temporal cortex (namely hV4, inferior occipital gyrus, posterior fusiform area and mid-fusiform area). They concluded that this increase in pRF size led to an increase in position tolerance which would facilitate the information process. Therefore, we can argue that the increased pRF sizes in response to triggered emotion can indicate the facilitation of visual processing. Additionally, our findings support the hypothesis of concurrent pathways of emotional and attentional modulations by showing the similar results with the attention studies.

We also found the pRF centers shifted towards the periphery in emotional condition compared to both scrambled and neutral condition. This pRF shift and the increased pRF size would lead to more overlapping pRFs in the visual system.

### 4.3 pRF sizes are larger in the right hemisphere than in the left hemisphere

It has been widely shown that the right hemisphere was affected more by emotion [62, 63] and attention [64] than the left hemisphere. It has been also suggested the lateralization of emotional processing such that the right hemisphere was more responsive to the negative emotions and the left hemisphere was more responsive to the positive emotions [65]. We also found that the effect of fearful stimulus on right hemisphere was more than that on left hemisphere. Our results support the lateralization of emotional processing.

Moreover, the pRF sizes on right hemisphere was estimated bigger than the pRF sizes on left hemisphere in all conditions. This difference was consistent among all the subjects even though we had one left-handed subject, which indicated that the handedness was irrelevant to the difference we found. This difference support the idea of hemispheric asymmetry. Some argued that right hemisphere processes global information or categorical information whereas left hemisphere processes local information or coordinate information [66]. The right hemisphere was suggested to have larger and overlapping receptive field for categorical processing whereas the left hemisphere should have smaller and non-overlapping receptive fields for coordinate processing by Kosslyn, Chabris and Chad in 1992 [67]. They suggested such a distinction between hemispheres according to their computational simulation based on the idea of hemispheric asymmetry. However, no direct evidences for the difference between pRF sizes of two hemispheres can be found in literature, although there are some studies supporting indirectly this idea [68], they could not show the hemispheric asymmetry. Our findings about the hemispheric asymmetry supports the idea that the right hemisphere has neurons with larger receptive fields than the neurons on left hemisphere.

The larger number of reliable vertices in right hemisphere than the left hemisphere might be related to the difference in pRF estimations. The larger pRF sizes in right hemisphere might indicate that the larger pRFs at more eccentric

side could be estimated better for right hemisphere than the left hemisphere. However, the comparison of the locations of pRF centers showed that the mean locations of pRF centers were not always more eccentric in right hemisphere compared to left hemisphere. Instead, the mean locations of pRF centers are different in left and right hemispheres and the direction of this difference can change from retinotopic region to region.

## 4.4 Conclusion

In this study, we examined the effect of the visual stimuli with emotional cues on pRF estimations. The emotional modulation on visual processing may facilitate the visual processing by providing an increased position tolerance. To move further, we can speculate that in a fearful condition, the content could be more important than the exact location of the fearful stimulus and therefore, the acuity can be compromised for the sake of more information about the source of fear.

We can also state that the emotion modulation can lead to the shift in pRF locations towards the eccentric side while the emotional cue was presented at the eccentricity. The pRF shift can be due to the more attention to the image with emotional cue. Moreover, it is clear that the effect of emotion is correlated with the individual differences. In addition to the findings about emotional modulation, we argue that using coherent images rather than random patterns might be better to map visual cortex by using the pRF estimation method.

Our study supported the hypothesis that two hemispheres process the information differently. We showed that the right hemisphere has larger pRFs than the left hemisphere. Moreover, the right hemisphere was more responsive to the fearful stimulus than the left hemisphere.

## 4.5 Limitations

In this study, we showed the change in pRF size by emotional modulation. We could suggest the anxiety level as the individual differences in the degree of emotional modulation because it has been shown that the anxiety level could affect the emotional modulation on visual processing [69, 70]. The individual differences can be investigated in further studies.

During the experiments, a small part of images was presented due to the nature of pRF stimulus. One can argue that the target emotion may not be triggered with such a small part of the image. Although it has been shown that a small part of image is enough to perceive the information [44], and the participant reported that they could understand the content of image while looking at the fixation point, we could not be certain about the triggered level of fear. One solution for this question can be to measure heart rate or pulse during the experiment for the further studies.

We argued that the coherent images were better to use as pRF stimulus by comparing the emotional and scrambled conditions. We could also perform a forth session with scrambled versions of neutral images in order to check whether similar difference between emotional condition and scrambled-emotional condition can be observed between neutral condition and scrambled-neutral condition. We could test the estimation power of coherent images better with a second scrambled condition. However, we did not perform an additional condition in order not to increase the duration of experiment.

## 4.6 Future directions

Our findings suggest that emotion affects the pRF sizes in ventral stream. The increase in pRF size can be due to a top-down modulation of emotion probably by amygdala. To investigate how the emotion can modulate the visual processing, the network can be studied by a functional connectivity analysis. Moreover,



the findings of our study and also of a further connectivity study can be applied to machine learning. We can model and predict the pRF sizes in response to the changes in emotional state. It would be useful to understand the emotional modulation on visual system, which is very important for some psychological disorders that affect the emotional state, such as anxiety, stress-related or bipolar disorders. People with such a psychological disorder might be affected differently by triggered emotion. The change in pRF sizes as a result of emotional modulation can be investigated also in people with anxiety, stress-related or bipolar disorders.

# Bibliography

- [1] F. Yildirim, J. Carvalho, and F. W. Cornelissen, “A second-order orientation-contrast stimulus for population-receptive-field-based retinotopic mapping,” *NeuroImage*, vol. 164, no. May, pp. 183–193, 2018.
- [2] B. de Haas and D. S. Schwarzkopf, “Spatially selective responses to Kanizsa and occlusion stimuli in human visual cortex,” *Scientific Reports*, vol. 8, no. 611, pp. 1–11, 2018.
- [3] D. He, C. Mo, Y. Wang, and F. Fang, “Position shifts of fMRI-based population receptive fields in human visual cortex induced by Ponzo illusion,” *Experimental Brain Research*, vol. 233, no. 12, pp. 3535–3541, 2015.
- [4] P. J. Lang, M. M. Bradley, J. R. Fitzsimmons, B. N. Cuthbert, J. D. Scott, B. Moulder, and V. Nangia, “Emotional arousal and activation of the visual cortex: An fMRI analysis,” *Psychophysiology*, vol. 35, no. 2, pp. 199–210, 1998.
- [5] H. T. Schupp, M. Junghofer, A. I. Weike, and A. O. Hamm, “Emotional facilitation of sensory processing in the visual cortex,” *Psychological Science*, vol. 14, no. 1, pp. 7–13, 2003.
- [6] S. O. Dumoulin and B. A. Wandell, “Population receptive field estimates in human visual cortex,” *NeuroImage*, vol. 39, no. 2, pp. 647–660, 2008.
- [7] C. S. Sherrington, “Observations on the scratch-reflex in the spinal dog,” *The Journal of Physiology*, vol. 34, no. 1-2, pp. 1–50, 1906.

- [8] H. K. Hartline, “The response of single optic nerve fibers of the vertebrate eye to illumination of the retina,” *American Journal of Physiology*, vol. 121, pp. 400–415, 1937.
- [9] D. Hubel and T. Wiesel, “Receptive fields of single neurones in the cat’s striate cortex,” *Journal of Physiology*, vol. 148, pp. 574–591, 1959.
- [10] E. Marg, J. E. Adams, and B. Rutkin, “Receptive fields of cells in the human visual cortex,” *Experientia*, vol. 24, no. 4, pp. 348–350, 1968.
- [11] S. W. Kuffler, “Discharge patterns and functional organization of mammalian retina,” *Journal of neurophysiology*, vol. 16, no. 1, pp. 37–68, 1953.
- [12] J. Bullier and T. T. Norton, “Comparison of receptive-field properties of X and Y ganglion cells with X and Y lateral geniculate cells in the cat,” *Journal of Neurophysiology*, vol. 42, no. 1, pp. 274–291, 1979.
- [13] E. R. Kandel, J. H. Schwartz, T. M. Jessel, S. A. Siegelbaum, and A. J. Hudspeth, eds., *Principles of neural science*. The McGraw-Hill Companies, Inc., 5 ed., 2013.
- [14] B. A. Wandell, S. O. Dumoulin, and A. A. Brewer, “Visual field maps in human cortex,” *Neuron*, vol. 56, no. 2, pp. 366–383, 2007.
- [15] L. G. Ungerleider and J. V. Haxby, “‘What’ and ‘where’ in the human brain,” *Current opinion in neurobiology*, vol. 4, pp. 157–165, 1994.
- [16] W. A. Press, A. A. Brewer, R. F. Dougherty, A. R. Wade, and B. A. Wandell, “Visual areas and spatial summation in human visual cortex,” *Vision Research*, vol. 41, no. 10-11, pp. 1321–1332, 2001.
- [17] A. C. Huk, R. F. Dougherty, and D. J. Heeger, “Retinotopy and functional subdivision of human areas MT and MST,” vol. 22, no. 16, pp. 7195–7205, 2002.
- [18] K. A. Hansen, K. N. Kay, and J. L. Gallant, “Topographic Organization in and near Human Visual Area V4,” *Journal of Neuroscience*, vol. 27, no. 44, pp. 11896–11911, 2007.

- [19] R. B. Tootell and N. Hadjikhani, "Where is 'Dorsal V4' in Human Visual Cortex? Retinotopic, Topographic and Functional Evidence," *Cerebral Cortex*, vol. 11, no. 4, pp. 298–311, 2001.
- [20] N. Hadjikhani, A. K. Liu, A. M. Dale, P. Cavanagh, and R. B. Tootell, "Retinotopy and color sensitivity in human visual cortical area V8," *Nature Neuroscience*, vol. 1, no. 3, pp. 235–335, 1998.
- [21] E. Goddard, D. J. Mannion, J. S. McDonald, S. G. Solomon, and C. W. G. Clifford, "Color responsiveness argues against a dorsal component of human V4," *Journal of Vision*, vol. 11, no. 4, pp. 3–3, 2011.
- [22] J. Larsson and D. J. Heeger, "Two Retinotopic Visual Areas in Human Lateral Occipital Cortex," *Journal of Neuroscience*, vol. 26, no. 51, pp. 13128–13142, 2006.
- [23] M. J. Arcaro, S. A. McMains, B. D. Singer, and S. Kastner, "Retinotopic organization of human ventral visual cortex.," *The Journal of neuroscience : the official journal of the Society for Neuroscience*, vol. 29, no. 34, pp. 10638–10652, 2009.
- [24] R. B. Tootell, N. Hadjikhani, E. K. Hall, S. Marrett, W. Vanduffel, J. T. Vaughan, and A. M. Dale, "The retinotopy of visual spatial attention," *Neuron*, vol. 21, no. 6, pp. 1409–1422, 1998.
- [25] J. D. Swisher, M. A. Halko, L. B. Merabet, S. A. McMains, and D. C. Somers, "Visual Topography of Human Intraparietal Sulcus," *Journal of Neuroscience*, vol. 27, no. 20, pp. 5326–5337, 2007.
- [26] S. A. Engel, G. H. Glover, and B. A. Wandell, "Retinotopic organization in human visual cortex and the spatial precision of functional MRI," *Cerebral Cortex*, vol. 7, pp. 181–192, 1997.
- [27] I. Alvarez, B. de Haas, C. A. Clark, G. Rees, and D. S. Schwarzkopf, "Comparing different stimulus configurations for population receptive field mapping in human fMRI," *Frontiers in Human Neuroscience*, vol. 9, no. 96, pp. 1–16, 2015.

- [28] E. J. Anderson, M. S. Tibber, D. S. Schwarzkopf, S. S. Shergill, E. Fernandez-Egea, G. Rees, and S. C. Dakin, “Visual population receptive fields in people with schizophrenia have reduced inhibitory surrounds,” *The Journal of Neuroscience*, vol. 37, no. 6, pp. 1546–1556, 2017.
- [29] R. M. Murray and S. W. Lewis, “Is schizophrenia a neurodevelopmental disorder?,” *British Medical Journal (Clinical research ed.)*, vol. 296, no. 6614, p. 63, 1988.
- [30] T. Dekker, D. S. Schwarzkopf, B. de Haas, M. Nardini, and M. I. Sereno, “Population receptive field tuning properties of visual cortex during childhood,” *Developmental Cognitive Neuroscience*, 2019.
- [31] G. Kanizsa, “Subjective Contours,” *Scientific American*, vol. 234, no. 4, pp. 48–53, 1976.
- [32] L. E. Welbourne, A. B. Morland, and A. R. Wade, “Population receptive field (pRF) measurements of chromatic responses in human visual cortex using fMRI,” *NeuroImage*, vol. 167, pp. 84–94, 2018.
- [33] P. Vuilleumier and J. Driver, “Modulation of visual processing by attention and emotion: Windows on causal interactions between human brain regions,” *Philosophical Transactions of the Royal Society B: Biological Sciences*, vol. 362, pp. 837–855, 2007.
- [34] T. C. Sprague and J. T. Serences, “Attention modulates spatial priority maps in the human occipital, parietal and frontal cortices,” *Nature Neuroscience*, vol. 16, no. 12, pp. 1879–1887, 2013.
- [35] T. Womelsdorf, K. Anton-Erxleben, F. Pieper, and S. Treue, “Dynamic shifts of visual receptive fields in cortical area MT by spatial attention,” *Nature Neuroscience*, vol. 9, no. 9, pp. 1156–1160, 2006.
- [36] P. Fries, J. H. Reynolds, A. E. Rorie, and R. Desimone, “Modulation of oscillatory neuronal synchronization by selective visual attention,” *Science*, vol. 291, pp. 1560–1563, 2001.

- [37] M. Watanabe, K. Cheng, Y. Murayama, K. Ueno, T. Asamizuya, K. Tanaka, and N. Logothetis, “Attention but not awareness modulates the BOLD signal in the human V1 during binocular suppression,” *Science*, vol. 334, pp. 829–831, 2011.
- [38] A. I. Jack, G. L. Shulman, A. Z. Snyder, M. Mcavoy, and M. Corbetta, “Separate modulations of human V1 associated with spatial attention and task structure,” *Neuron*, vol. 51, pp. 135–147, 2006.
- [39] D. G. Amaral, H. Behniea, and J. L. Kelly, “Topographic organization of projections from the amygdala to the visual cortex in the macaque monkey,” *Neuroscience*, vol. 118, pp. 1099–1120, 2003.
- [40] J. L. Freese and D. G. Amaral, “Synaptic organization of projections from the amygdala to visual cortical areas TE and V1 in the macaque monkey,” *Journal of Comparative Neurology*, vol. 496, no. 5, pp. 655–667, 2006.
- [41] K. Amano, B. A. Wandell, and S. O. Dumoulin, “Visual field maps, population receptive field sizes, and visual field coverage in the human MT+ complex,” *Journal of neurophysiology*, vol. 102, no. 5, pp. 2704–18, 2009.
- [42] J. A. van Dijk, B. de Haas, C. Moutsiana, and D. S. Schwarzkopf, “Intersession reliability of population receptive field estimates,” *NeuroImage*, vol. 143, pp. 293–303, 2016.
- [43] M. Riegel, Ł. Żurawski, M. Wierzba, A. Moslehi, Ł. Klocek, M. Horvat, A. Grabowska, J. Michałowski, K. Jednoróg, and A. Marchewka, “Characterization of the Nencki Affective Picture System by discrete emotional categories (NAPS BE),” *Behavior Research Methods*, vol. 48, no. 2, pp. 600–612, 2016.
- [44] W. Zuiderbaan, B. M. Harvey, and S. O. Dumoulin, “Image identification from brain activity using the population receptive field model,” *PLoS ONE*, vol. 12, no. 9, pp. 1–17, 2017.
- [45] D. H. Brainard, “The Psychophysics Toolbox,” *Spatial Vision*, vol. 10, pp. 433–436, 1997.

- [46] A. M. Dale, B. Fischl, and M. I. Sereno, "Cortical surface-based analysis I: Segmentation and surface reconstruction," *NeuroImage*, vol. 9, no. 2, pp. 179–194, 1999.
- [47] B. Fischl, M. I. Sereno, and A. M. Dale, "Cortical surface-based analysis II: Inflation, flattening, and a surface-based coordinate system.," *NeuroImage*, vol. 9, no. 2, pp. 195–207, 1999.
- [48] D. L. Collins, P. Neelin, T. M. Peters, and A. C. Evans, "Automatic 3D intersubject registration of MR volumetric data in standardized Talairach space," *Journal of Computer Assisted Tomography*, vol. 18, no. 2, pp. 192–205, 1994.
- [49] B. Fischl and A. M. Dale, "Measuring the thickness of the human cerebral cortex from magnetic resonance images," *Proceedings of the National Academy of Sciences*, vol. 97, no. 20, pp. 11044–11049, 2000.
- [50] B. Fischl, A. Liu, and A. M. Dale, "Automated manifold surgery: Constructing geometrically accurate and topologically correct models of the human cerebral cortex," *IEEE Transactions on Medical Imaging*, vol. 20, no. 1, pp. 70–80, 2001.
- [51] B. Fischl, D. H. Salat, E. Busa, M. Albert, M. Dieterich, C. Haselgrove, A. van Der Kouwe, R. Killiany, D. Kennedy, S. Klaveness, A. Montillo, N. Makris, B. Rosen, and A. M. Dale, "Whole brain segmentation: Automated labeling of neuroanatomical structures in the human brain," *Neuron*, vol. 33, no. 3, pp. 341–355, 2002.
- [52] B. Fischl, A. van Der Kouwe, C. Destrieux, E. Halgren, F. Ségonne, D. H. Salat, E. Busa, L. J. Seidman, J. Goldstein, D. Kennedy, V. Caviness, N. Markis, B. Rosen, and A. M. Dale, "Automatically parcellating the human cerebral cortex," *Cerebral Cortex*, vol. 14, pp. 11–22, 2004.
- [53] Bruce Fischl, Martin I. Sereno, Roger B.H. Tootell, and Anders M. Dale, "High-resolution inter-subject averaging and a coordinate system for the cortical surface," *Human Brain Mapping*, vol. 8, no. 4, pp. 272–284, 1999.

- [54] “Statistical Parametric Mapping,” 2014.
- [55] D. S. Schwarzkopf, B. de Haas, and I. Alvarez, “SamSrf 6 - Toolbox for pRF modelling,” 2018.
- [56] J. Harel, C. Koch, and P. Perona, “Graph-Based Visual Saliency Jonathan,” in *Conference on Neural Information Processing Systems*, 2006.
- [57] G. Rainer, M. Augath, T. Trinath, and N. K. Logothetis, “Nonmonotonic noise tuning of BOLD fMRI signal to natural images in the visual cortex of the anesthetized monkey,” *Current Biology*, vol. 11, pp. 846–854, 2001.
- [58] J. Touryan, G. Felsen, and Y. Dan, “Spatial structure of complex cell receptive fields measured with natural images,” *Neuron*, vol. 45, no. 5, pp. 781–791, 2005.
- [59] D. Smyth, B. Willmore, G. E. Baker, I. D. Thompson, and D. J. Tolhurst, “The receptive-field organization of simple cells in primary visual cortex of ferrets under natural scene stimulation.,” *The Journal of Neuroscience*, vol. 23, no. 11, pp. 4746–4759, 2003.
- [60] S. O. Murray, D. Kersten, B. A. Olshausen, P. Schrater, and D. L. Woods, “Shape perception reduces activity in human primary visual cortex,” *Proceedings of the National Academy of Sciences*, vol. 99, no. 23, pp. 15164–15169, 2002.
- [61] K. N. Kay, K. S. Weiner, and K. Grill-Spector, “Attention reduces spatial uncertainty in human ventral temporal cortex,” *Current Biology*, vol. 25, no. 5, pp. 595–600, 2015.
- [62] G. L. Ahern and G. E. Schwartz, “Differential lateralization for positive versus negative emotion,” *Neuropsychologia*, vol. 17, no. 6, pp. 693–698, 1979.
- [63] W. Heller, J. B. Nitschke, and G. A. Miller, “Lateralization in emotion and emotional disorders,” *Current Directions in Psychological Science*, vol. 7, no. 1, pp. 26–32, 1998.



- [64] M. Wang, X. Wang, L. Xue, D. Huang, and Y. Chen, “Visual attention modulates the asymmetric influence of each cerebral hemisphere on spatial perception,” *Scientific Reports*, vol. 6, no. January, pp. 1–8, 2016.
- [65] E. Beraha, J. Eggers, C. Hindi Attar, S. Gutwinski, F. Schlagenhaut, M. Stoy, P. Sterzer, T. Kienast, A. Heinz, and F. Bermpohl, “Hemispheric Asymmetry for Affective Stimulus Processing in Healthy Subjects-A fMRI Study,” *PLoS ONE*, vol. 7, no. 10, pp. 1–9, 2012.
- [66] J. B. Hellige, “Hemispheric asymmetry for visual information processing,” *Acta Neurobiologiae Experimentalis*, vol. 56, no. 1, pp. 485–497, 1996.
- [67] S. M. Kosslyn, C. F. Chabris, and C. J. Marsolek, “Categorical versus coordinate spatial relations: computational analyses and computer simulations,” *American Psychological Association*, vol. 18, no. 2, pp. 562–577, 1992.
- [68] S. M. Kosslyn, A. K. Anderson, L. A. Hillger, and S. E. Hamilton, “Hemispheric Differences in Sizes of Receptive Fields or Attentional Biases?,” *Neuropsychology*, vol. 8, no. 2, pp. 139–147, 1994.
- [69] J. Yiend and A. Mathews, “Anxiety and attention to threatening pictures,” *The Quarterly Journal of Experimental Psychology*, vol. 54A, no. 3, pp. 665–681, 2012.
- [70] E. Fox, “Processing emotional facial expressions: The role of anxiety and awareness,” *Cognitive, Affective and Behavioral Neuroscience*, vol. 2, no. 1, pp. 52–63, 2002.

# Appendix A

## Behavioral Test for Image Recognition

We presented the stimulus movie for neutral and emotional conditions to 3 of the participants. After the stimulus presentation, we asked them which images they have seen during the experiment with a multiple-choice test (which can be found in Appendix A). Additionally, we ask them if they experienced any emotional change.

The stimulus presentation was the same with the fMRI experiments as described above. Participants were seated 65 cm in front of a 30-inch NEC Multi-Sync LCD monitor (LCD3090WQXi; 60 Hz refresh rate;  $1920 \times 1200$  screen resolution) in a dark room. They were presented counter-clockwise rotating wedge and expanding ring followed by clockwise rotating wedge and contracting ring for neutral and emotional images. Then, they answered the multiple-choice test prepared specifically for our images. The test included 60 items. 12 of the items were not presented in any of the conditions. 13 items were emotion-related and 36 items were neutral-related. 1 item (“human”) was both emotion- and neutral-related. We calculated the ratio of correct answers by dividing the number of answers to the number of items for that condition. We eliminated the unrelated answers such as television since there was no images including television or any

similar device for both conditions.

The average ratio of correct answers was 79% for emotional condition whereas it was 41% for neutral condition. The individual results were shown in Table A.1 The reason for this difference can be the increased variety in neutral condition. The emotional images included several images of soldiers and wild animals whereas the neutral images had a variety of images such as vehicles, trees, building and several objects. As a result, we can argue that the participants could recognize the content of stimulus.

Additionally, we ask them if they experienced any emotional change. The participants reported that they did not feel anything during both the neutral and the emotional experiment. However, they noted that the images in emotional condition were uncomfortable and little disgusting.

Table A.1: The ratio of correct answers of each subjects for test of image recognition

	Neutral	Emotional
Subject 2	56%	92%
Subject 3	53%	92%
Subject 4	14%	54%
Average	41%	79%

**Katılımcı:**

**Tarih:**

**Cinsiyet:**

**Çalışma:**

**Yaş:**

Aşağıdaki soruları, az önce katıldığınız deneydeki görsel uyarınları düşünerek yanıtlayınız.

**1. Deney sırasında aşağıdaki görsellerden hangisini/hangilerini gördünüz?**

<input type="checkbox"/>	Yarasa	<input type="checkbox"/>	Banyo	<input type="checkbox"/>	Çocuk
<input type="checkbox"/>	Saat	<input type="checkbox"/>	Asker	<input type="checkbox"/>	Bina
<input type="checkbox"/>	Hasta	<input type="checkbox"/>	Ayak	<input type="checkbox"/>	Deniz
<input type="checkbox"/>	Kaplan	<input type="checkbox"/>	Klavye	<input type="checkbox"/>	Bacak
<input type="checkbox"/>	Balık	<input type="checkbox"/>	Dikiş makinesi	<input type="checkbox"/>	Köpek
<input type="checkbox"/>	Timsah	<input type="checkbox"/>	Vinç	<input type="checkbox"/>	Direk
<input type="checkbox"/>	Kuş	<input type="checkbox"/>	Lamba	<input type="checkbox"/>	Kurt
<input type="checkbox"/>	Otobüs	<input type="checkbox"/>	Şemsiye	<input type="checkbox"/>	Köpek balığı
<input type="checkbox"/>	Çöp kovası	<input type="checkbox"/>	Gemi	<input type="checkbox"/>	Cephane
<input type="checkbox"/>	Bardak	<input type="checkbox"/>	Bavul	<input type="checkbox"/>	İnsan
<input type="checkbox"/>	Tuvalet	<input type="checkbox"/>	Gözlük	<input type="checkbox"/>	Motosiklet
<input type="checkbox"/>	Sandalye	<input type="checkbox"/>	Gökyüzü	<input type="checkbox"/>	Bisiklet
<input type="checkbox"/>	Oyuncak ördek	<input type="checkbox"/>	Radyo	<input type="checkbox"/>	Tekerlek
<input type="checkbox"/>	Teleferik	<input type="checkbox"/>	Çanta	<input type="checkbox"/>	Araba
<input type="checkbox"/>	Yılan	<input type="checkbox"/>	İnsan	<input type="checkbox"/>	Kablo
<input type="checkbox"/>	Sürahi	<input type="checkbox"/>	Ağaç	<input type="checkbox"/>	Taş
<input type="checkbox"/>	Tarla	<input type="checkbox"/>	Silah	<input type="checkbox"/>	Leopar
<input type="checkbox"/>	Telefon	<input type="checkbox"/>	Ayakkabı	<input type="checkbox"/>	Çim biçme makinesi
<input type="checkbox"/>	Pedal	<input type="checkbox"/>	Toprak	<input type="checkbox"/>	Keman
<input type="checkbox"/>	Televizyon	<input type="checkbox"/>	Maymun	<input type="checkbox"/>	Tencere

**2. Deney sırasında herhangi bir duygusal değişim hissettiniz mi? Evet ise tarif edin.**

# Appendix B

## Saliency Maps of Images

We used Graph-Based Visual Saliency to create saliency maps of images [56]. This model finds the attracting or salient points. The color codes were used to indicate the most salient point with red and the least salient point with blue. We rendered the saliency maps onto gray squares since we could not publicly share the images because of the ethical issues. The saliency maps of scrambled images were shown in Figure B.1. The saliency maps of neutral images were shown in Figure B.2. The saliency maps of emotional images were shown in Figure B.3. Images were labelled with numbers to be followed easily. However, the order of images was randomized at the beginning of each run.

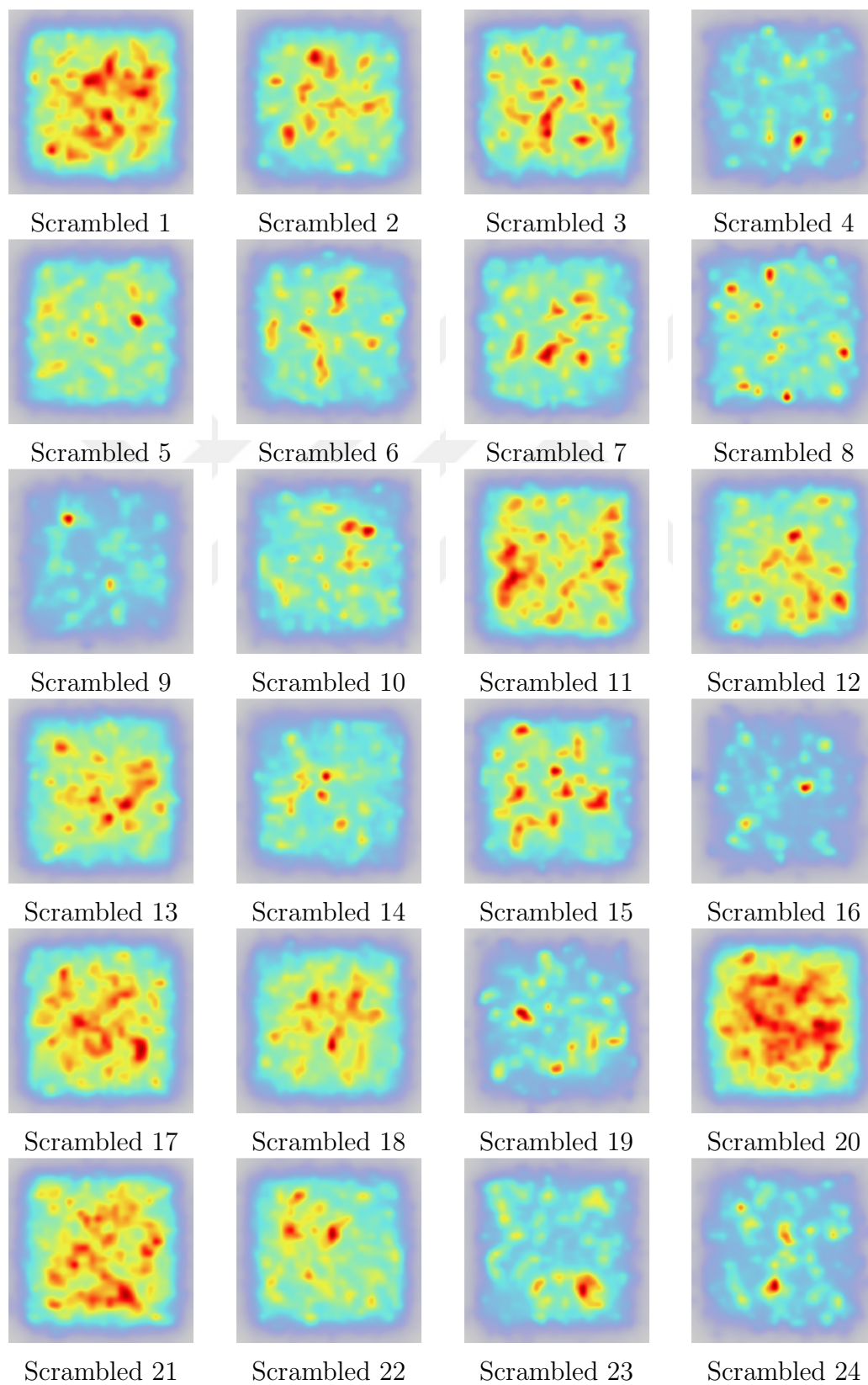
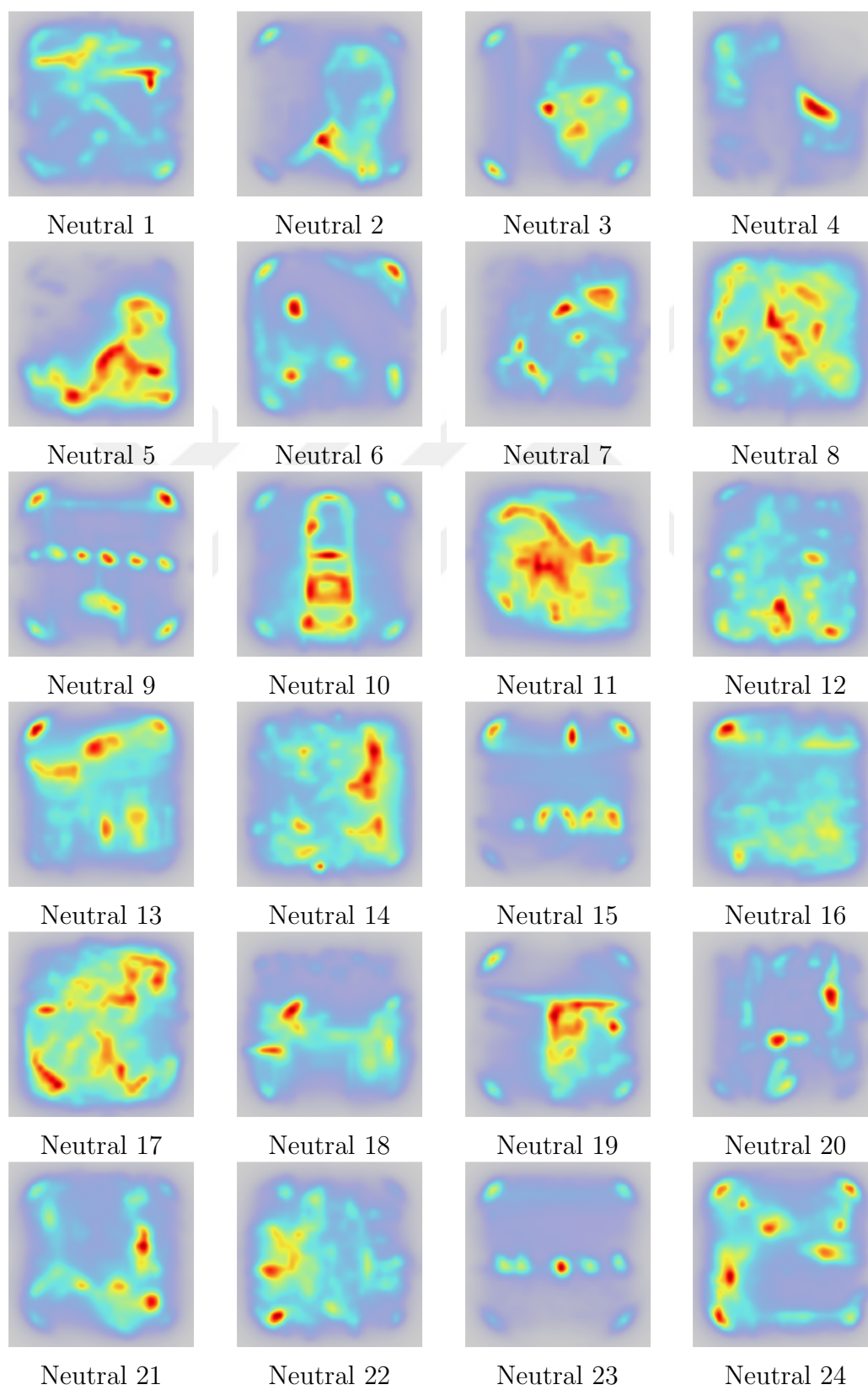
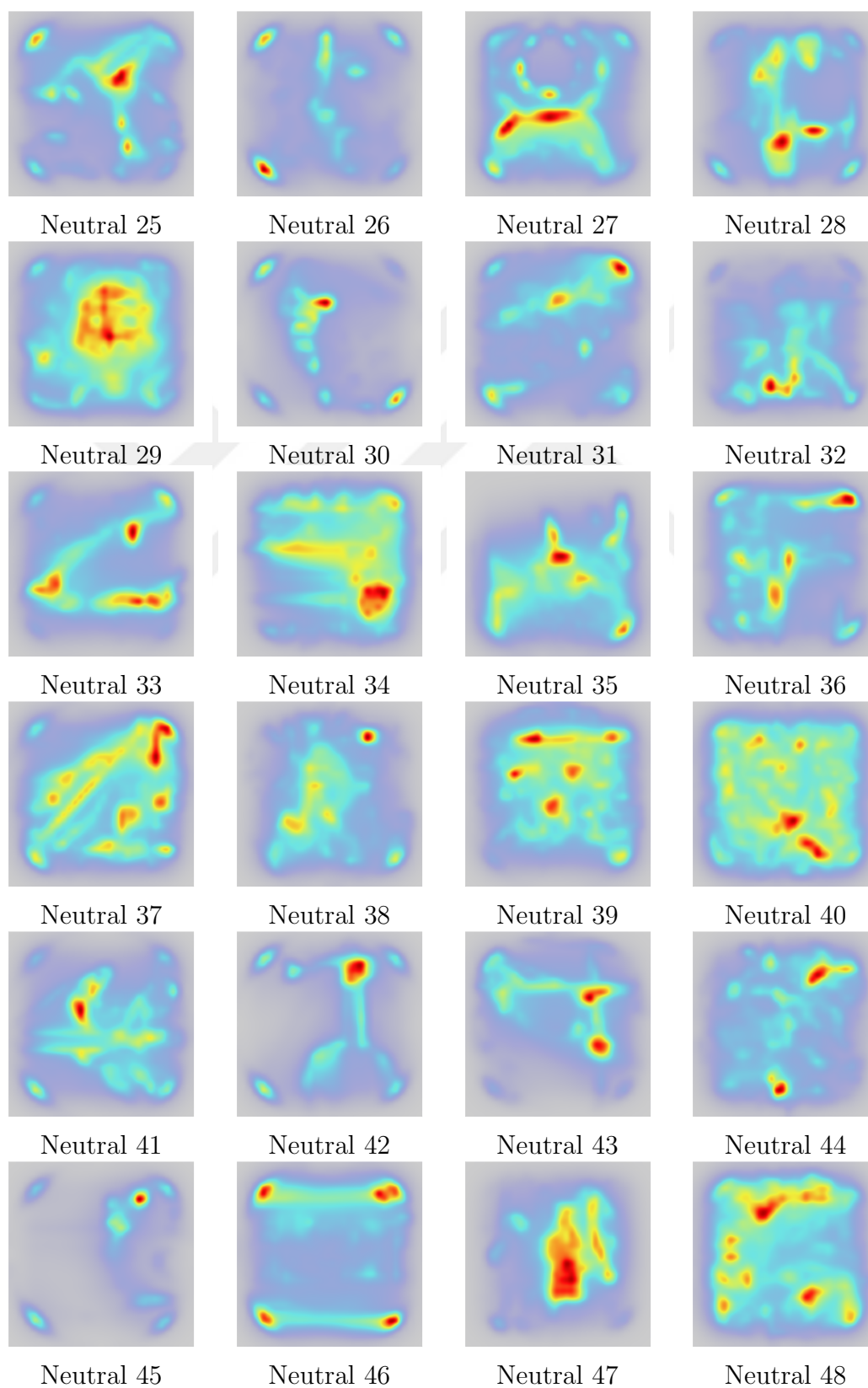


Figure B.1: The saliency maps of scrambled images







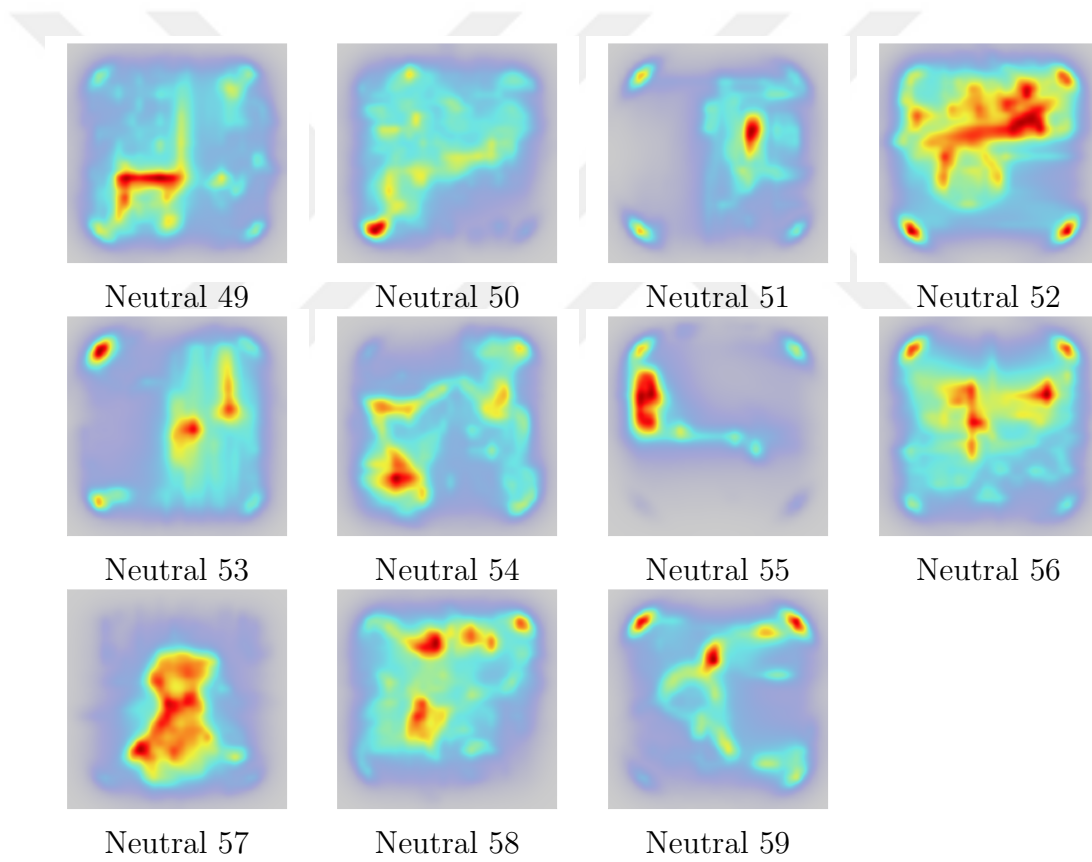


Figure B.2: The saliency maps of neutral images

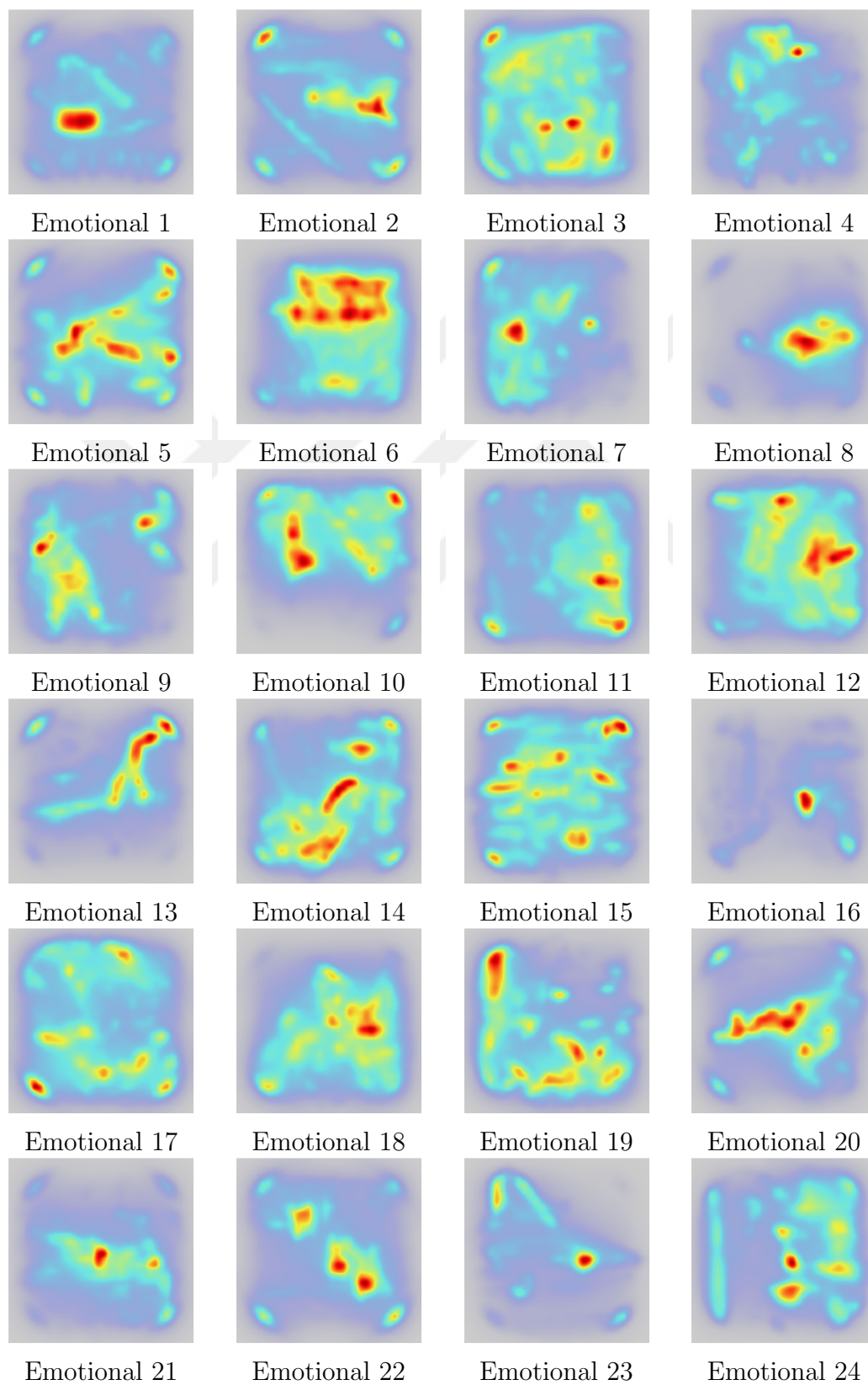


Figure B.3: The saliency maps of emotional images

# Appendix C

## Within-Subject Results

We analyzed the responses to fixation task by correlating the time when fixation point changed its color and the response time. Then, we correlated the color of fixation point and the response of the subjects. The results are presented in separate tables for each subject. According to the results, the attentional difference in MR scans were negligible.

The descriptive plots for pRF estimations of subjects are given in Figures C.1, C.3, C.5, C.7 and C.9. There is a strong hemispheric asymmetry in each subject's data. The difference between pRF estimations of emotional and neutral conditions on right hemisphere was significant whereas there was almost no difference between the pRF estimations of those two conditions on left hemisphere. Moreover, the difference between emotional and scrambled conditions were consistent on both hemispheres. In general, the pRF sizes on right hemisphere is larger than the pRF sizes of left hemisphere.

## C.1 Subject 1

Gender: F

Age: 28

Table C.1: Success of Subject 1 in fixation task.

Run #	Scrambled	Neutral	Emotional
1	.9806	.9877	.9679
2	1.000	.9876	.9944
3	.9040	.9615	.9777
4	.9581	.9939	.9745
5	.9877	.9819	.9805
6	.9940	.9944	.9944
7	.9824	.9938	.9806
8	.9934	.9859	.9708
9	.9857	.9942	.9892
10	.9760	.9932	.9873
11	.9865	.9799	.9941
12	.9937	.9935	.9812
Average	.9860	.9873	.9827

*Note.* The ratio of correct answers of Subject 1 for fixation task.

Table C.2: Precision of Subject 1 in fixation task.

Run #	Scrambled	Neutral	Emotional
1	.3825	.6886	.5863
2	-.1574	.6328	.5341
3	.8108	.7889	.2146
4	.1974	.5750	.6380
5	.6515	.7377	.6487
6	-.1992	.5944	1.6125
7	.6737	.5997	.5872
8	.6969	.5626	.6816
9	.6971	.6033	-.2773
10	-.3885	.3429	.2814
11	.7885	.8868	.3441
12	.3134	.3861	-.4245
Average	.3722	.6166	.4522

*Note.* The averaged delay in response (in seconds) of Subject 1. Negative values mean that the mistaken responses of subject when there was no event was a lot.

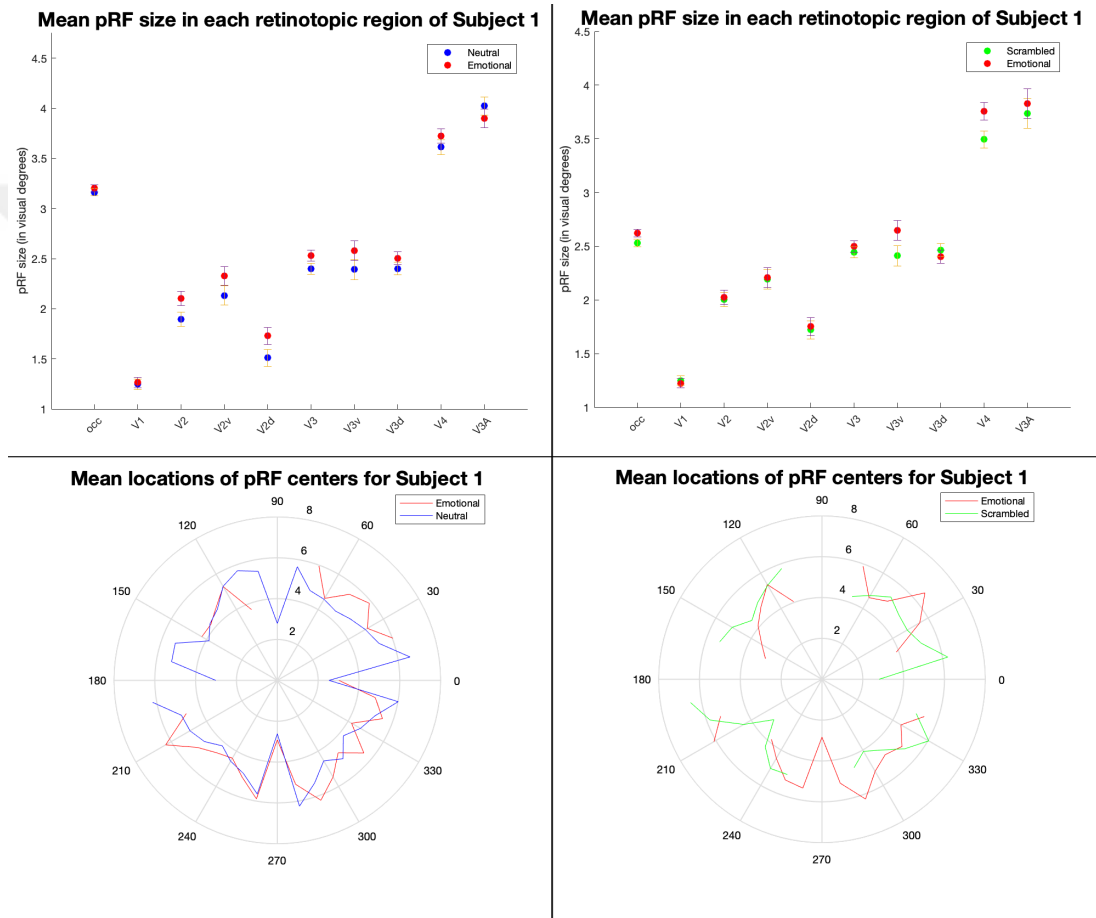


Figure C.1: **The pRF estimates for Subject 1.** The locations of pRF centers were calculated by using the estimated  $X_0$  and  $Y_0$  values at the reliable vertices in scrambled, neutral and emotional conditions. The lines on the mean locations of pRF centers graphs represent the mean of the calculated values for the locations of pRF centers at each polar coordinate. The points on the pRF size graphs represent the mean of the estimated sigma values in each ROI. The red color represents the emotional data, the blue color represents the neutral data and the green color represents the scrambled data. The error bars indicate the 95% confidence interval.

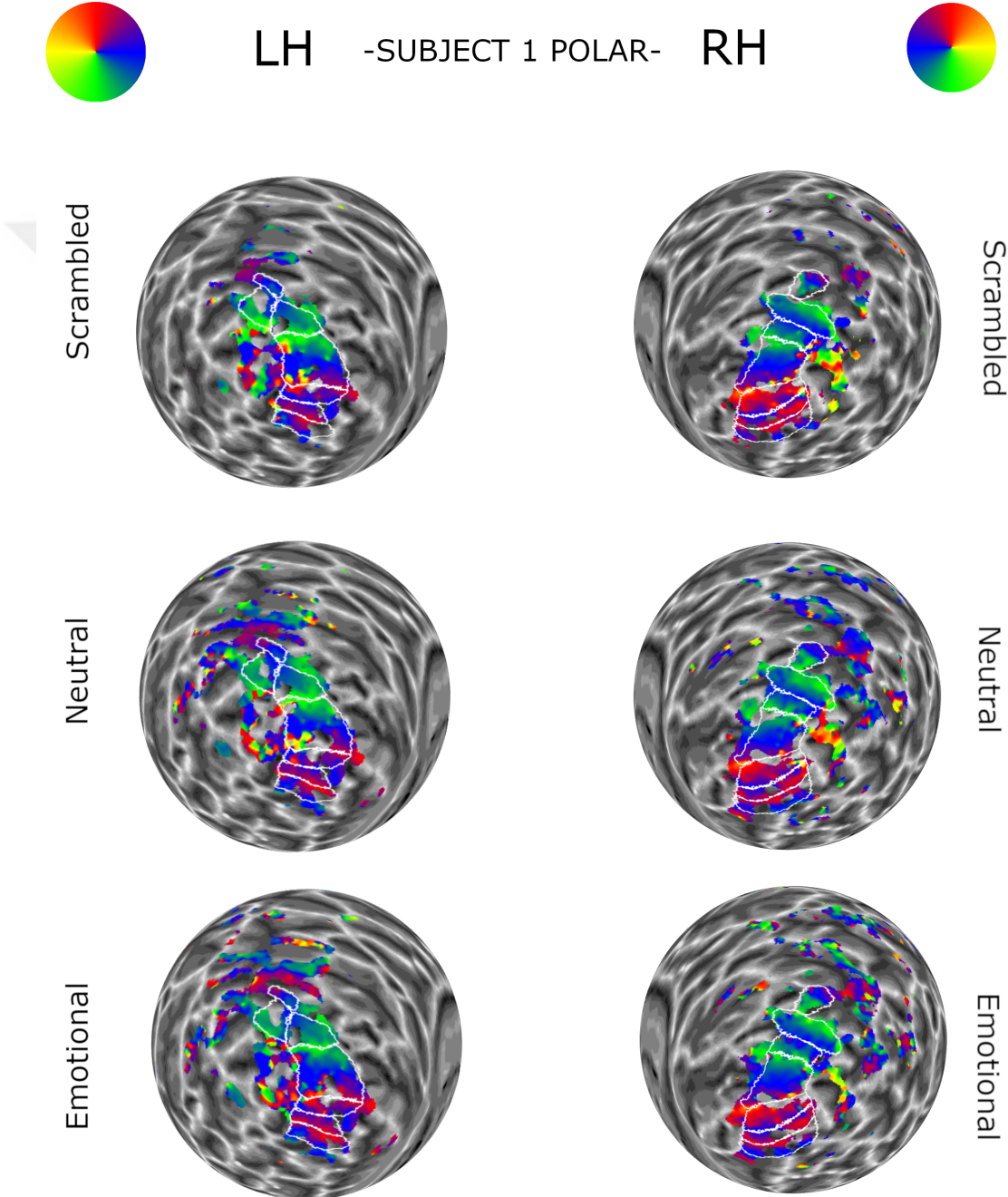


Figure C.2: **Polar maps of Subject 1.** The circular legend indicates the corresponding color for each polar angle. The borders of retinotopic regions were labeled on the maps. <sup>c2</sup>HB: eccentricity maps?

## C.2 Subject 2

Gender: M

Age: 27

Table C.3: Success of Subject 2 in fixation task.

Run #	Scrambled	Neutral	Emotional
1	.9941	.9714	.9861
2	.9104	1.000	.9934
3	.9514	.9554	.9641
4	.9814	.9803	.9720
5	.9592	.8534	.9379
6	.9521	.9739	.9083
7	.9928	.9394	.9565
8	.9925	.9545	.9359
9	.9796	.8881	.9429
10	.9689	1.000	.9236
11	.9929	.9556	.9718
12	.9533	.9913	.9866
Average	.9690	.9553	.9566

*Note.* The ratio of correct answers of Subject 2 for fixation task.



Table C.4: Precision of Subject 2 in fixation task.

Run #	Scrambled	Neutral	Emotional
1	.7690	1.0308	.9434
2	.6780	.2710	.3138
3	1.6092	1.3347	.6624
4	.5001	.3824	.4492
5	.9482	1.3639	.7262
6	.2530	.5792	.8559
7	1.1589	7.7776	.9430
8	.4907	.4844	.6182
9	.7590	1.2762	.7088
10	-.0165	.8896	.6350
11	1.1675	1.3056	.8962
12	.4349	2.1707	.3963
Average	.7293	1.5722	.6790

*Note.* The averaged delay in response (in seconds) of Subject 2. Negative values mean that the mistaken responses of subject when there was no event was a lot.

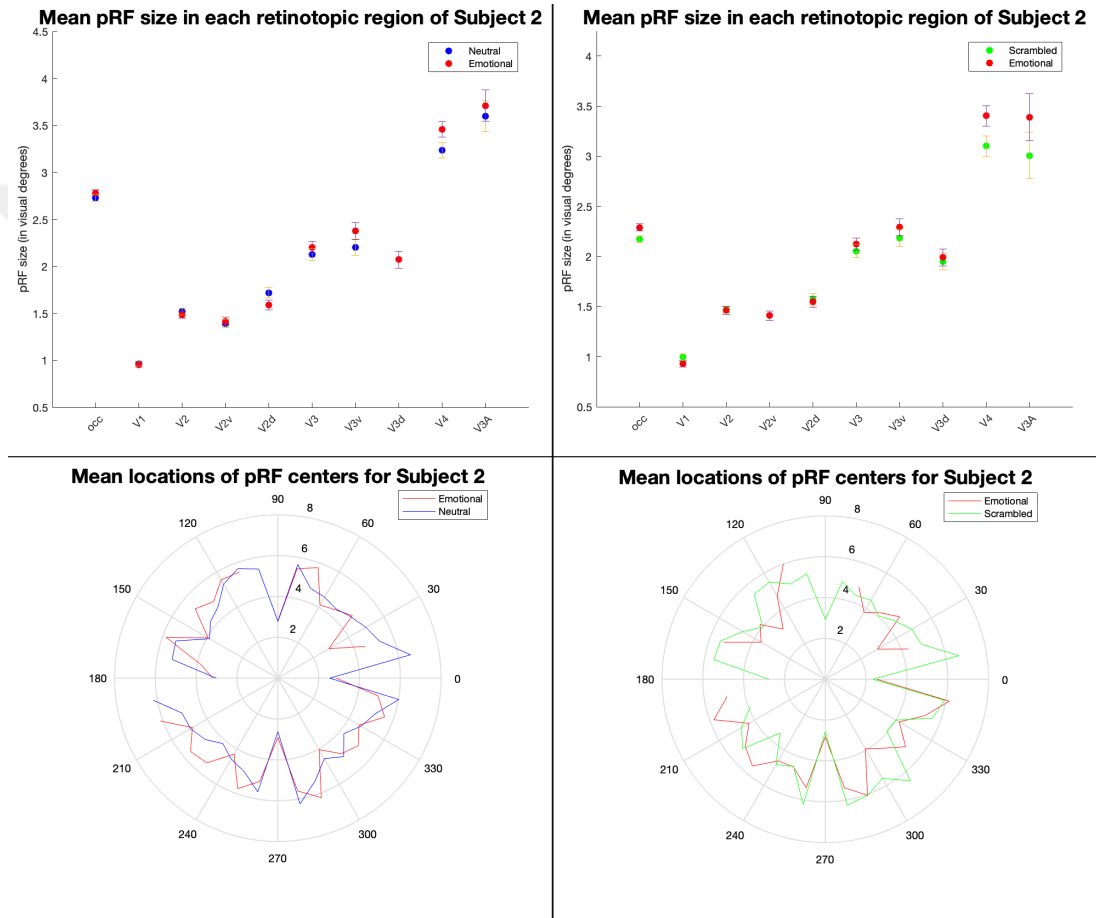


Figure C.3: **The pRF estimates for Subject 2.** The locations of pRF centers were calculated by using the estimated  $X_0$  and  $Y_0$  values at the reliable vertices in scrambled, neutral and emotional conditions. The lines on the mean locations of pRF centers graphs represent the mean of the calculated values for the locations of pRF centers at each polar coordinate. The points on the pRF size graphs represent the mean of the estimated sigma values in each ROI. The red color represents the emotional data, the blue color represents the neutral data and the green color represents the scrambled data. The error bars indicate the 95% confidence interval.

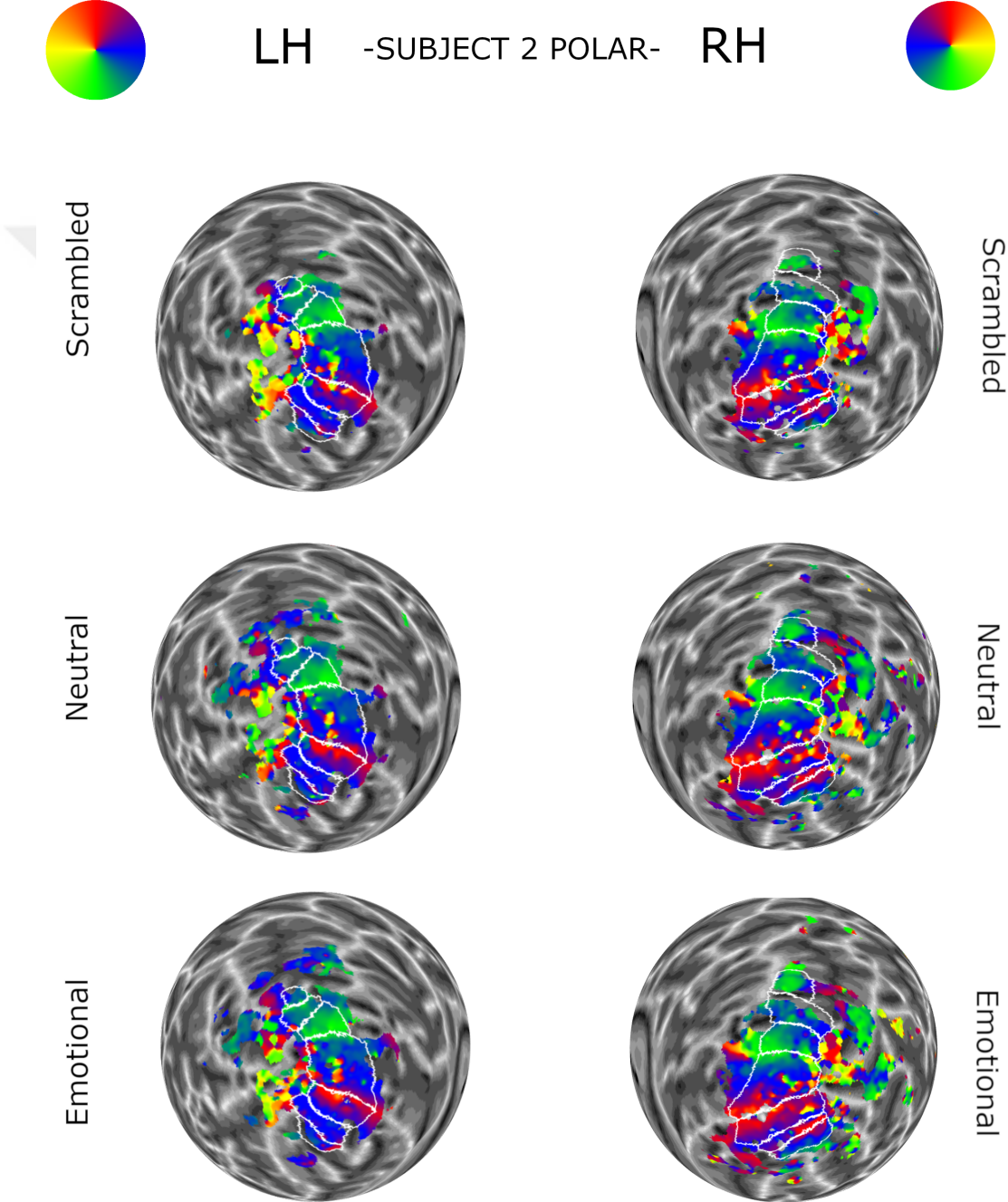


Figure C.4: **Polar maps of Subject 2.** The circular legend indicates the corresponding color for each polar angle. The borders of retinotopic regions were labeled on the maps.

### C.3 Subject 3

Gender: F

Age: 26

Table C.5: Success of Subject 3 in fixation task.

Run #	Scrambled	Neutral	Emotional
1	1.000	.9933	1.000
2	.9571	.9301	.9933
3	.9883	.9851	.9809
4	.9725	.9615	.9824
5	.9497	.9859	.9940
6	1.000	.9503	.9931
7	.9655	.9820	.9632
8	.9767	.9593	.9932
9	.9779	.9942	.9938
10	.9862	.9688	.9712
11	1.000	.9577	.9612
12	1.000	.9877	.9932
Average	.9812	.9713	.9850

*Note.* The ratio of correct answers of Subject 3 for fixation task.

Table C.6: Precision of Subject 3 in fixation task.

Run #	Scrambled	Neutral	Emotional
1	.8205	.6836	.4135
2	.6319	.6890	.4323
3	.1674	.1972	.8424
4	.5765	-.0861	.4721
5	.6304	.3154	.0780
6	.4458	-.0367	.7769
7	.8548	.8969	.7222
8	.4700	-.6162	.2251
9	.3168	.5805	.5268
10	.1755	.3320	.2030
11	.5502	1.0154	.5504
12	.3076	.4866	.5794
Average	.4956	.3715	.4852

*Note.* The averaged delay in response (in seconds) of Subject 3. Negative values mean that the mistaken responses of subject when there was no event was a lot.

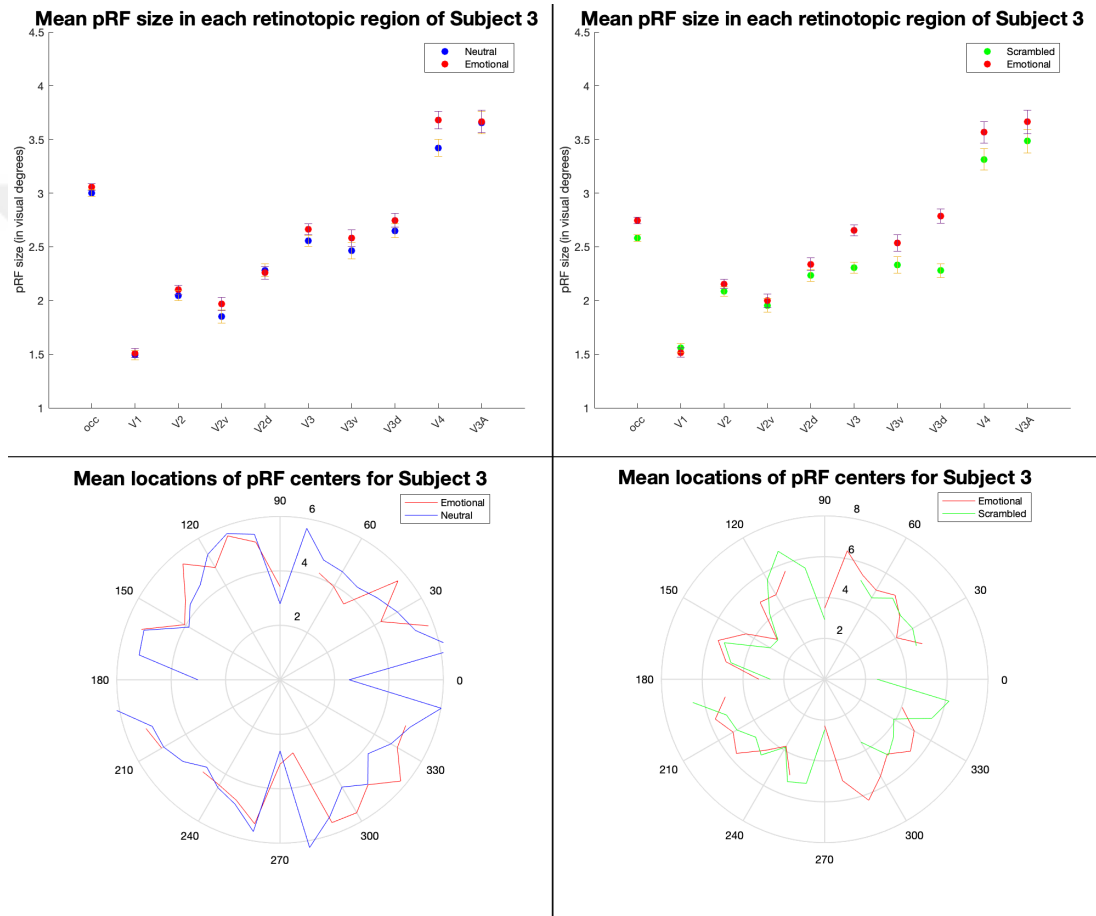


Figure C.5: **The pRF estimates for Subject 3.** The locations of pRF centers were calculated by using the estimated  $X_0$  and  $Y_0$  values at the reliable vertices in scrambled, neutral and emotional conditions. The lines on the mean locations of pRF centers graphs represent the mean of the calculated values for the locations of pRF centers at each polar coordinate. The points on the pRF size graphs represent the mean of the estimated sigma values in each ROI. The red color represents the emotional data, the blue color represents the neutral data and the green color represents the scrambled data. The error bars indicate the 95% confidence interval.

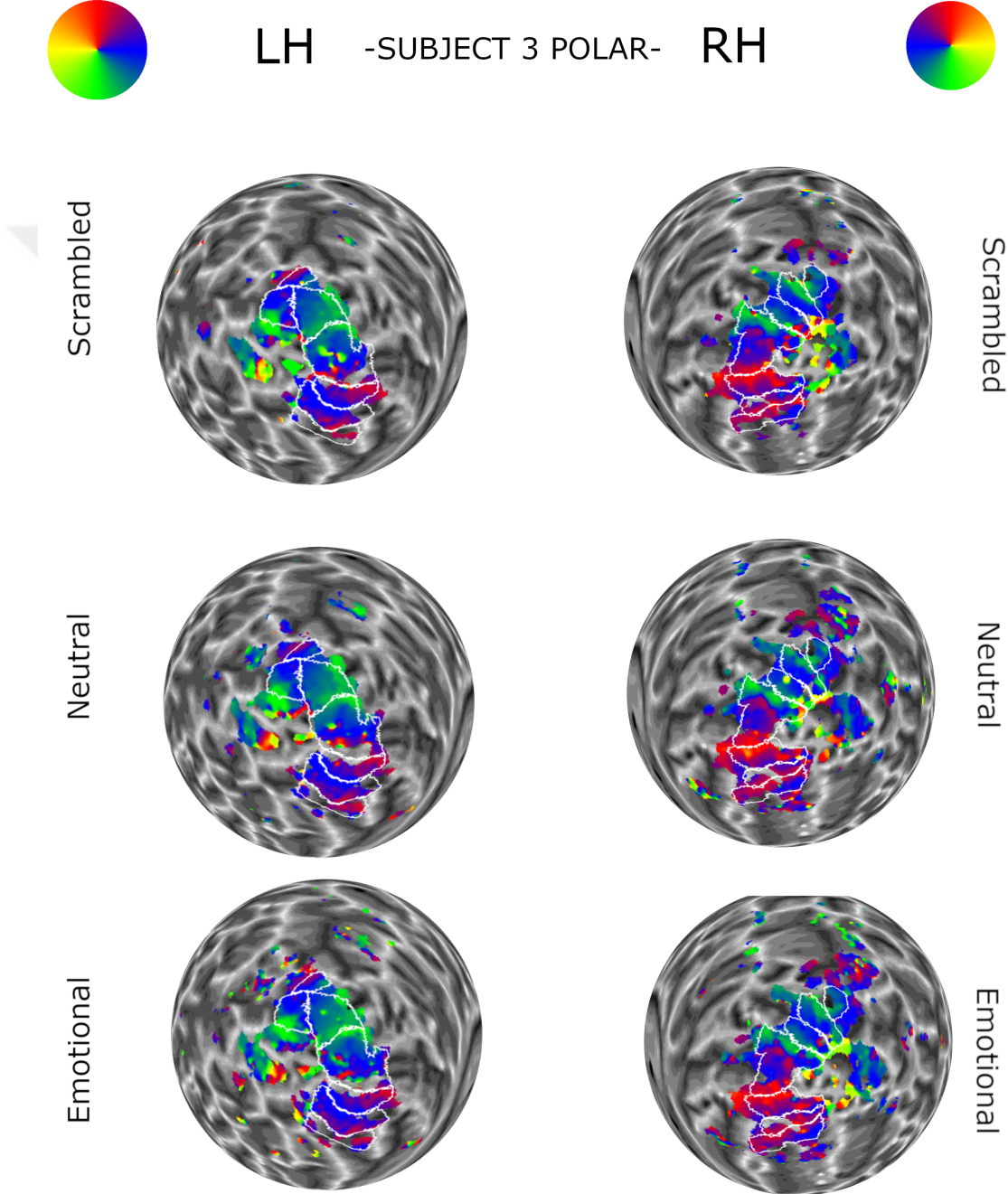


Figure C.6: **Polar maps of Subject 3.** The circular legend indicates the corresponding color for each polar angle. The borders of retinotopic regions were labeled on the maps.

## C.4 Subject 4

Gender: M

Age: 26

Table C.7: Success of Subject 4 in fixation task.

Run #	Scrambled	Neutral	Emotional
1	.9917	.8421	.9024
2	1.000	.9872	.9496
3	.9844	.9350	.9151
4	.9627	.9858	.9492
5	.9508	.9638	.9619
6	.9552	.9444	.9505
7	.9869	.9545	.8500
8	.9848	.9412	.8600
9	.9924	.8689	.8880
10	.9236	.9027	.9149
11	.9030	.7870	.7368
12	.9304	.9065	.6839
Average	.9638	.9183	.8802

*Note.* The ratio of correct answers of Subject 4 for fixation task.



Table C.8: Precision of Subject 4 in fixation task.

Run #	Scrambled	Neutral	Emotional
1	.9235	6.7181	3.6993
2	.2701	-.5222	3.0295
3	2.3371	1.1918	17.1845
4	1.3248	-.0643	6.0792
5	1.8125	.3863	19.7666
6	-.2931	2.4904	1.6910
7	1.0446	3.6237	26.6333
8	.1499	1.8950	19.1762
9	2.1478	3.0239	28.1706
10	.5169	3.1018	-1.0501
11	2.1270	48.3748	61.3657
12	.9379	6.5506	95.3950
Average	1.1083	6.3975	23.4284

*Note.* The averaged delay in response (in seconds) of Subject 4. Negative values mean that the mistaken responses of subject when there was no event was a lot.

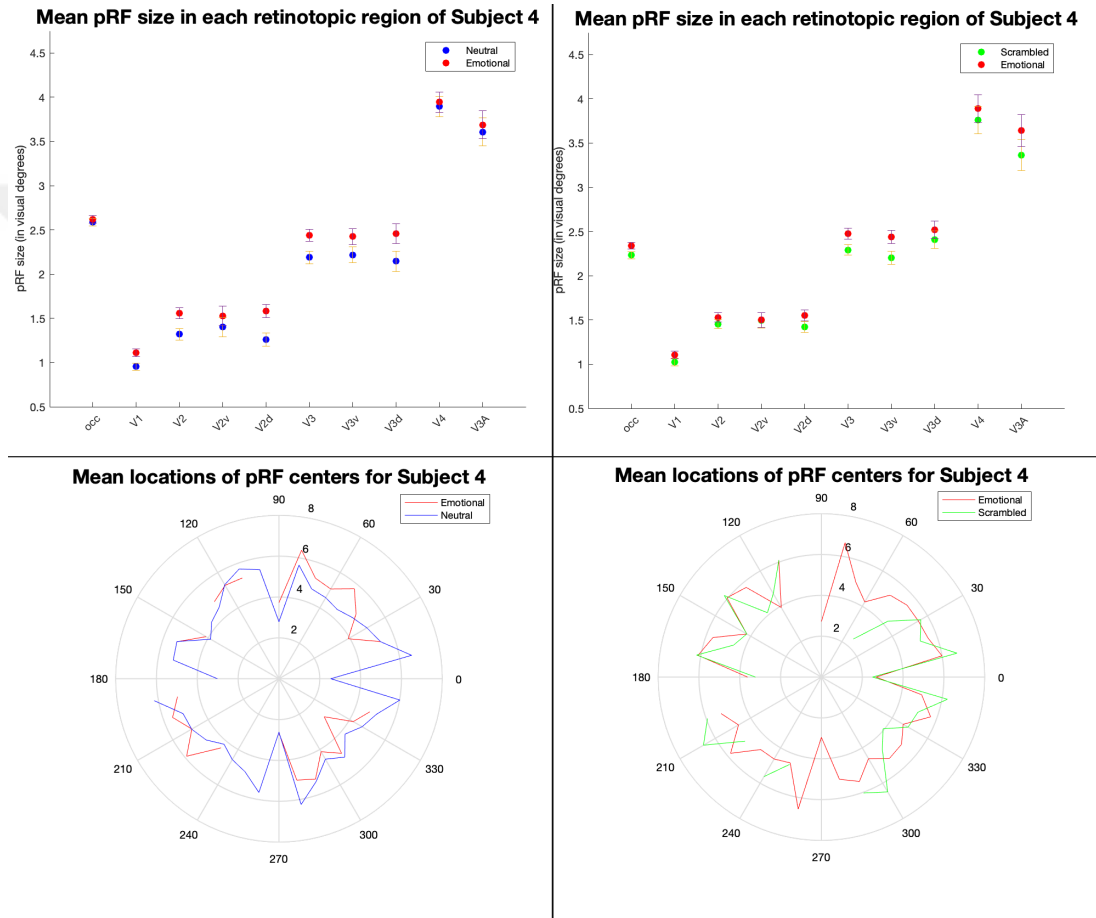


Figure C.7: **The pRF estimates for Subject 4.** The locations of pRF centers were calculated by using the estimated  $X_0$  and  $Y_0$  values at the reliable vertices in scrambled, neutral and emotional conditions. The lines on the mean locations of pRF centers graphs represent the mean of the calculated values for the locations of pRF centers at each polar coordinate. The points on the pRF size graphs represent the mean of the estimated sigma values in each ROI. The red color represents the emotional data, the blue color represents the neutral data and the green color represents the scrambled data. The error bars indicate the 95% confidence interval.

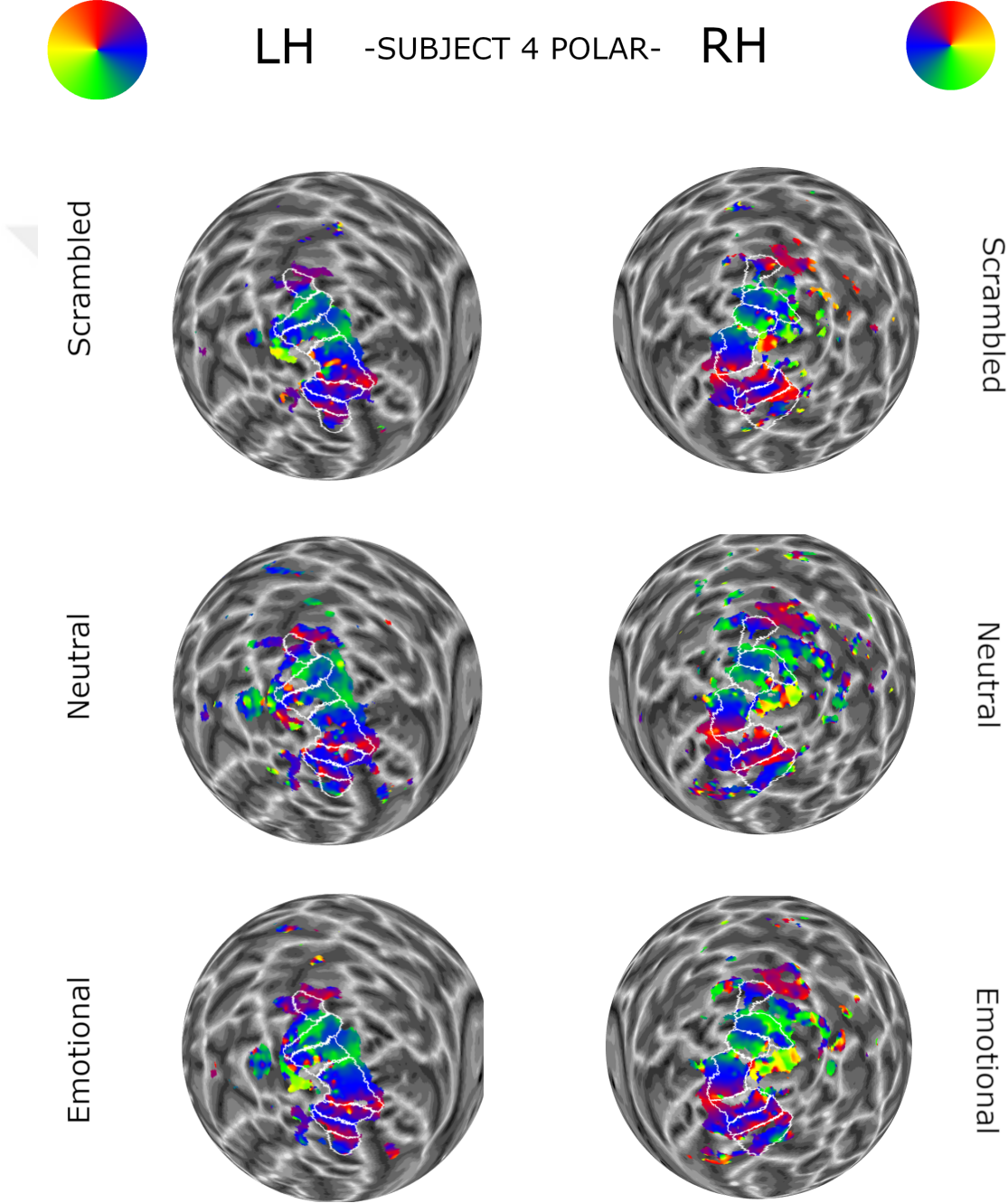


Figure C.8: **Polar maps of Subject 4.** The circular legend indicates the corresponding color for each polar angle. The borders of retinotopic regions were labeled on the maps.

## C.5 Subject 5

Gender: F

Age: 28

Table C.9: Success of Subject 5 in fixation task.

Run #	Scrambled	Neutral	Emotional
1	.9880	.9938	.9752
2	1.000	.9869	.9871
3	.9750	.9737	.9935
4	.9591	.9817	.9868
5	.9933	.9742	.9868
6	.9925	.9821	.9943
7	.9630	.9878	.9712
8	.9940	1.000	.9940
9	.9877	.9939	.9936
10	.9895	.9940	.9872
11	1.000	.9880	1.000
12	.9940	.9796	.9883
Average	.9863	.9863	.9882

*Note.* The ratio of correct answers of Subject 4 for fixation task.

Table C.10: Precision of Subject 5 in fixation task.

Run #	Scrambled	Neutral	Emotional
1	.8672	.2887	.4701
2	.0598	.2233	-.1188
3	.9424	1.0926	.8155
4	.1973	.2845	.2428
5	.7454	.5273	.3954
6	.1249	.2457	.3214
7	.2641	.6909	.5405
8	-.4740	-.0384	.4770
9	.6800	-.3609	.6556
10	.0532	-.4772	-.0710
11	.5783	.6171	.6996
12	.6942	.4233	-1.0223
Average	.3944	.2931	.2838

*Note.* The averaged delay in response (in seconds) of Subject 5. Negative values mean that the mistaken responses of subject when there was no event was a lot.

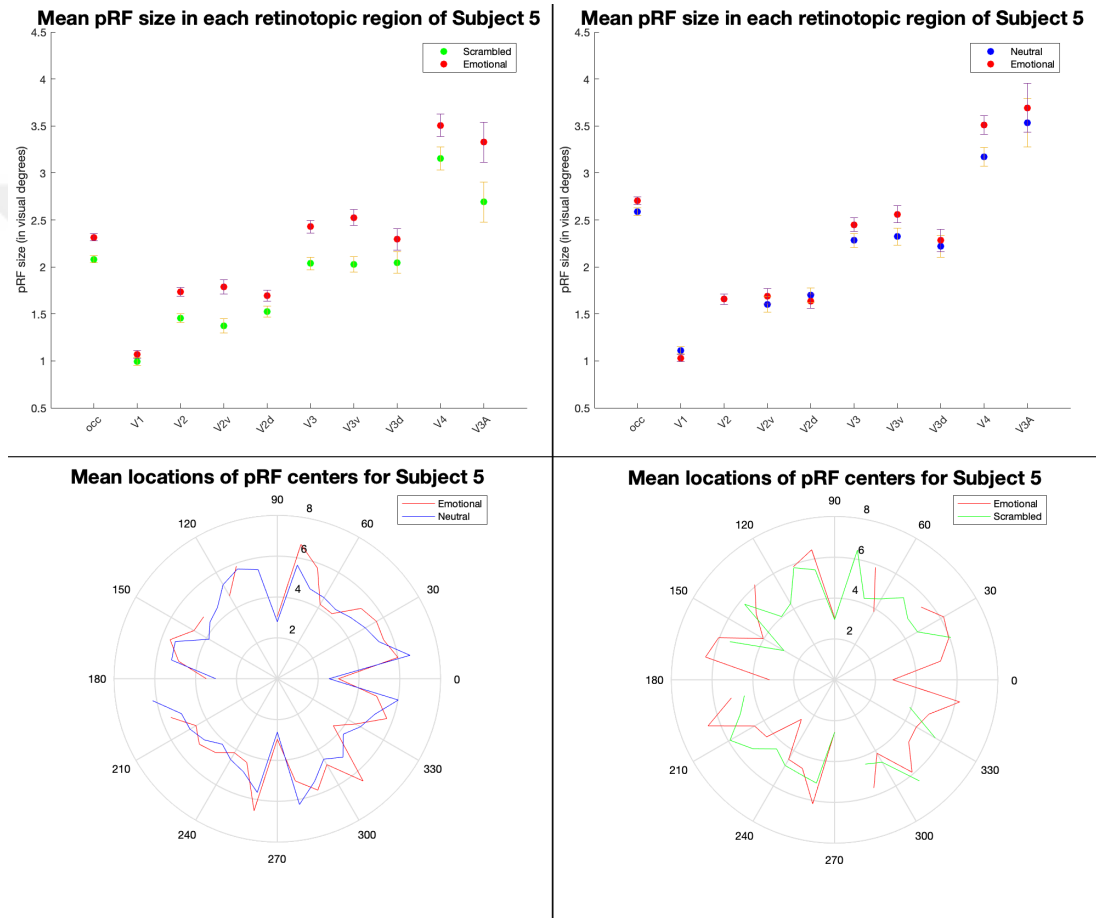


Figure C.9: **The pRF estimates for Subject 5.** The locations of pRF centers were calculated by using the estimated  $X_0$  and  $Y_0$  values at the reliable vertices in scrambled, neutral and emotional conditions. The lines on the mean locations of pRF centers graphs represent the mean of the calculated values for the locations of pRF centers at each polar coordinate. The points on the pRF size graphs represent the mean of the estimated sigma values in each ROI. The red color represents the emotional data, the blue color represents the neutral data and the green color represents the scrambled data. The error bars indicate the 95% confidence interval.

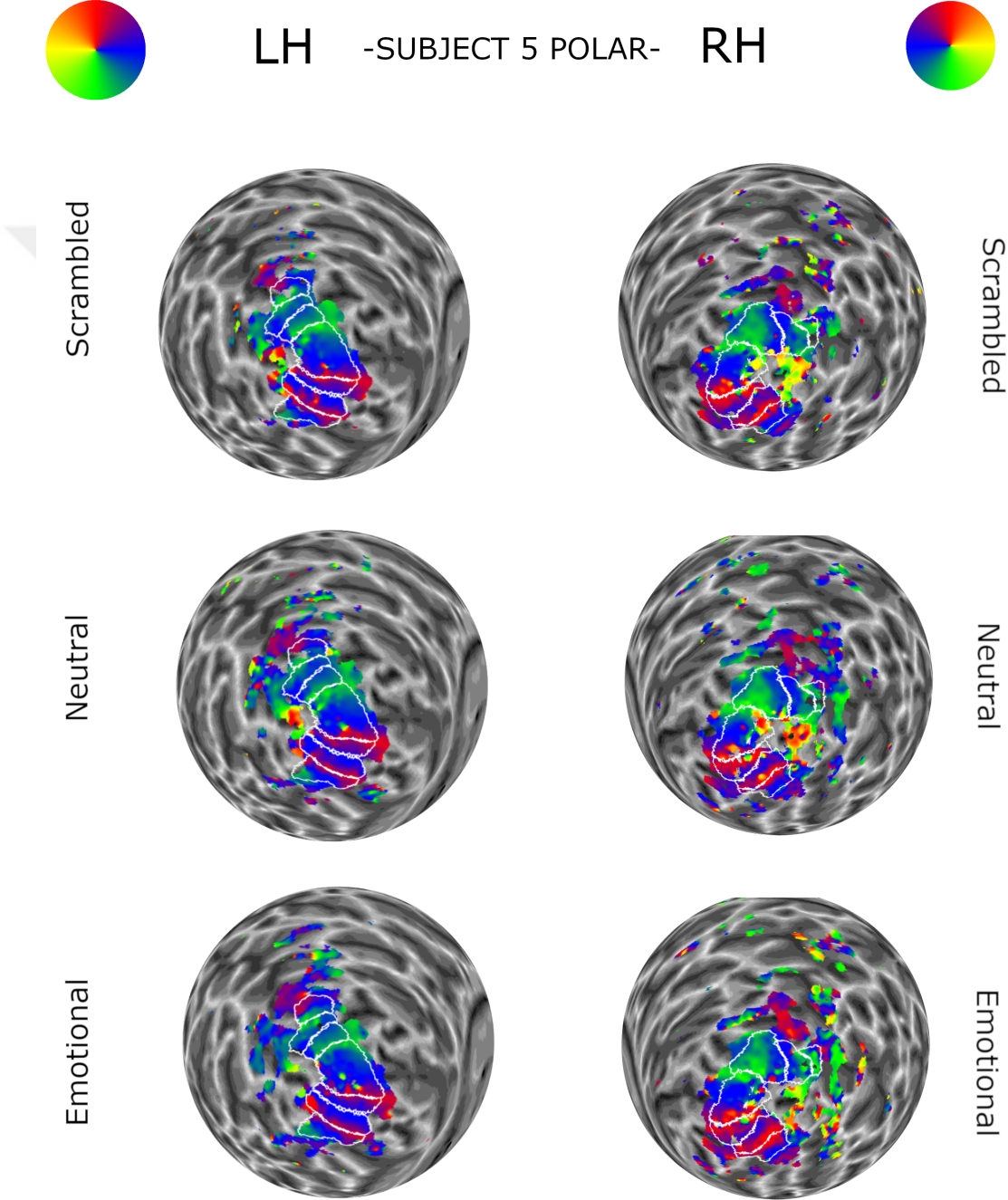


Figure C.10: **Polar maps of Subject 5.** The circular legend indicates the corresponding color for each polar angle. The borders of retinotopic regions were labeled on the maps.